Optical Microsensors And Microprobes

Chapter · January 1999

CITATIONS
17

READS
72

4 authors, including:

Gerhard Alfred Holst
PCO AG
57 PUBLICATIONS **1,368** CITATIONS
SEE PROFILE

Ingo Klimant
Graz University of Technology
224 PUBLICATIONS **8,482** CITATIONS
SEE PROFILE

Michael Kühl
University of Copenhagen
351 PUBLICATIONS **10,732** CITATIONS
SEE PROFILE

7. OPTICAL MICROSENSORS AND MICROPROBES

GERHARD HOLST, I. KLIMANT, MICHAEL KÜHL and OLIVER KOHLS

7.1 INTRODUCTION

Biogeochemical processes in the ocean are (to a large extent) regulated by the physico-chemical characteristics of the microenvironment where the processes occur. In the pelagic, phytoplankton, bacteria and small grazers interact and regulate the productivity in response to environmental variables like temperature, salinity or availability of nutrients and trace elements. Hot spots of metabolic activities are found in aggregates of microalgae or e.g. in planktonic foraminifera or radiolaria harbouring microalgal symbionts. Also, during the continuous export of biomass (e.g. dead or dying phytoplankton, faecal material and other organic debris) from the euphotic zone of the ocean, ca. 0.5–5 mm large aggregates (marine snow) are formed that are rapidly mineralised during their journey to the sea floor. In the open ocean, recycling of carbon and other essential elements thus mainly takes place in the water column, while only refractory material reaches the seafloor, where it is slowly degraded and buried. The deep sea sediment is thus a major sink for carbon on a global scale.

In coastal waters with shallower depths, an increasing amount of the pelagic production reaches the sea floor and causes more intense remineralisation in the sediment. This pelagic-benthic coupling is replaced in waters where sufficient light reaches the sea floor, by photosynthetic production in the upper sediment layers. Production and remineralisation become closely coupled in these photosynthetic sediments, and occur within a few mm thick overlapping reaction zones in the top layers of the sediment (Figure 7.1). In the extreme case of biofilms and microbial mats, this leads to extremely productive communities fuelled by microbenthic phototrophs, which partly rely on an efficient recycling of carbon and nutrients via heterotrophic microbes in their immediate neighbourhood. Here the complete range of production and remineralisation processes, usually found over *a* > 1 km deep water column and the sediment in the open ocean, are compressed to a few millimetres.

In marine aggregates and photosynthetic sediments, production and mineralisation processes are closely coupled and take place in a densely populated structured microenvironment of cells and exopolymers. The high volumetric conversion rates in these systems, in combination with the fact that hydrodynamic and diffusive boundary layers form at the interface between the system and the turbulent surrounding water phase, result in the formation of steep gradients of physico-chemical variables over spatial distances of $< 0.1-1$ mm. There can be steep gradients of light intensity and spectral composition due to intense scattering and absorption in the matrix of pigmented cells, exopolymers, and

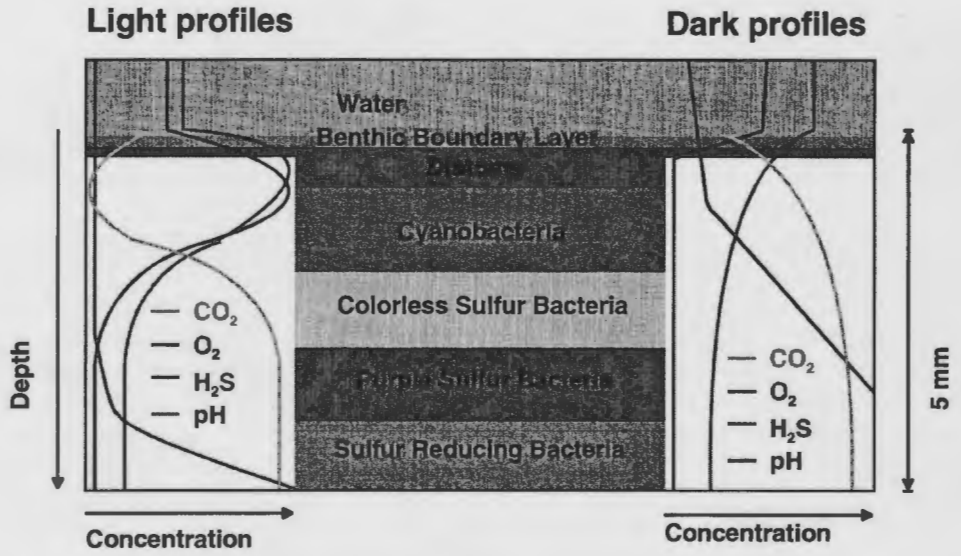

Figure 7.1 Vertical zonation of microbial mats and shallow water sediments. Typical concentration profiles of O_2, pH, CO_2 and H_2S vs. penetration depth are given for day (light profiles) and night (dark profiles) reflecting the photsynthetic activity of the upper layers.

mineral grains. Furthermore, there can be gradients of metabolic substrates/products like oxygen, carbon dioxide, hydrogen sulphide, methane, pH, nutrients and dissolved organic compounds.

Gradients are also present in deep-sea sediments, but due to the refractory quality of available organic material the gradients over the diffusive boundary layer and within the sediment are not as steep as in shallower waters. While oxygen penetration is less than 0.5 mm in the most active sediments, oxygen penetrates to greater than 50 cm in cold deep-sea sediments. Important exceptions from this general observation are the hydrothermal vents and seeps found in tectonically active areas of the deep sea. In these areas, dense and active benthic communities develop on the basis of geothermally fed chemolithotrophic microbes.

In all systems, many of the gradients result from mass transfer and metabolic activity. Provided that (non- or minimally-invasive) measurements at high spatial and temporal resolution can be performed, it is, therefore, possible to obtain detailed information about relevant transport processes, their interaction with the consumption/production of substrates/products, and the zonation and magnitude of the various conversion processes.

Such information is very important to understand the dynamics and regulation of biogeochemical processes in the ocean. Most traditional techniques in biogeochemistry are essentially "black box" approaches, where measured conversion

rates rely on assumptions about the actual microenvironment, where the processes occur. Using microprobes, these assumptions can be investigated and, if necessary, modified according to experimental information determined within the microenvironment.

The theme of this chapter is a description of one class of miniature measuring devices, fibre-optic microsensors, that allow such high resolution measurements to be performed either in the laboratory or directly in the ocean via use of special remote operating vehicles. We focus on technical aspects of instrumentation, sensor construction and performance. Only a few applications are described. Information about electrochemical microsensors and further examples of microsensor application can found in other chapters of this book and in some recent reviews (e.g. Revsbech and Jørgensen, 1986; Revsbech, 1994; Kühl *et al.*, 1994a; Kühl and Revsbech, 1998; Amann and Kühl, 1998).

7.2 OPTICAL MICROSENSORS AND MICROPROBES

Fibre optical devices and instrumentation for fine scale measurements of physicochemical variables in the aquatic environment typically operate to a spatial resolution of < 0.1 mm. It is important to discriminate between fibre optic microprobes that collect optical information from the medium surrounding the measuring fibre tip and direct it to a detector system, and fibre optic microsensors, microoptodes, that measure a chemical or physical variable via a reversible change in the optical properties of an indicator which is immobilized at the measuring fibre tip. Both types of devices are based on the use of single strand optical fibres for directing light information to and from the site of measurement. Optical fibres and optical components like fibre couplers and switches have been tremendously improved by the advancements in telecommunication industry and they display: low weight, robustness, immunity to electromagnetic radiation, high temperature stability and many other advantageous characteristics for use in measuring systems (Dakin and Culshaw, 1988). Due to the rapid progress of optoelectronics, many classical spectroscopic techniques can now be applied to measurements with small and easy to handle instruments. Especially, the current availability of robust fibre optical components and compatible light sources and detectors presents a huge advancement for the design of optical measuring systems. This has resulted in a large number of fibre optical sensors and sensor systems in recent years, and this development seems to be accelerating (Dakin and Culshaw, 1988; Wolfbeis, 1991). Most practical applications of such sensors have been realised in medicine and biotechnology, while the development and use of fibre optic sensors in environmental applications has been more limited. Nevertheless, fibre optic microprobes and microoptodes have seen numerous applications in oceanography, limnology, and biogeochemistry. (Kühl and Revsbech, 1998; Klimant *et al.*, 1997).

7.3 OPTICAL MICROSENSORS, MICROOPTODES

7.3.1 Spectroscopic Principles of Optical Sensing

Principally every interaction between light and matter which exhibits a reproducible and reversible sensitivity to a chemical or physical variable can be used to detect this variable. In this part we focus on the basics of spectroscopic principles used in microoptodes that use appropriate dye materials, which interacts with the analyte to be measured. Most of the experiences with such interactions exist in the visible part of the spectrum – which ranges from approximately 390 to 730 nm, and the processes and principles used in microoptodes mainly exploit this part of the electromagnetic spectrum.

The energy of the light can interact with the outer electrons of dye molecules with large electron systems. The π-electron system plays a key role. On the atomic scale, the molecular structure (and therefore the optical properties) of the dye are changed by either a chemical reaction or a change to its molecular environment. This can be due to protonation/deprotonation, oxidation/reduction or the presence of special kind of species. In any case, energy of incident light has to be absorbed by the dye, which only can happen if the energy levels within the molecular system exactly correspond to the incident light energy level.

In the Jablonski diagram (energy level scheme, Figure 7.2) the dye molecule is promoted from the electronic ground state S_0 to an excited level S_1 respectively

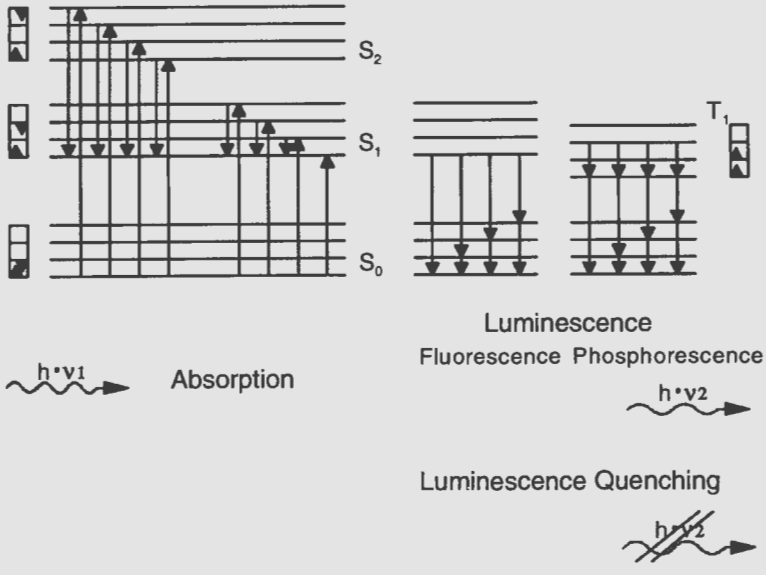

Figure 7.2 Jablonski diagram (energy level scheme) with the energetic ground level S_1, the excited singlet levels S_1 and S_2, and an excited triplet level T_1 ($h\nu$ = energy of light radiation).

S_2 depending on the light energy. The energy levels can be split into different sub-levels due to various possible rotational and vibrational energy levels of the molecule. The dye excitation/absorption spectrum thus consists of a huge amount of single energy transition processes.

Many dyes exhibit relaxation to the ground state S_0 via repetitive energy transfer to rotational and vibrational levels (as we can see in the Jablonski diagram between the excited levels S_1 and S_2 in Figure 7.2). These dyes are called absorption dyes. Fibre optical sensors, which have the dye immobilised at the fibre tip measure absorption indirectly, via the reflected and backscattered light from the fibre tip. In section 2.2.4 such an absorption dye based pH microsensor is described, where the protonated and the deprotonated form of the dye exhibit different absorption spectra.

Other dyes return to the ground level by emission of a photon. The photon usually has less energy than the absorbed photon, due to vibrational relaxation prior to photon emission. Therefore, the emission spectra of these dyes are shifted towards the red part of the spectrum as compared to the excitation spectrum, this effect is called the Stokes shift. If there is no intersystem crossing between the excited levels, the time between absorption and emission of a photon is very short (in the range of nanoseconds). In this case we talk about fluorescence. If there is intersystem crossing between triplet (T_1) and singlet (S_1) levels in the excited state, the relaxation process takes much longer, seconds to minutes. Here we talk about phosphorescence. Phosphorence only occurs when a strong internal interaction in the dye molecule is present. This is found, for instance, in some large metallo-organic molecules like platinum- or palladium-porphyrins. Both processes, fluorescence and phosphorescence, are also called luminescence.

Luminescence dyes enable measurements at wavelengths different from absorption because both are influenced by the analyte. In many applications this improves the efficiency of measurement. Some molecules, oxygen for example, are able to absorb energy from the excited dye by collision. The dye returns to the ground state without emitting a photon. The luminescence is quenched as a function of the amount of quenching molecules present. The quenching phenomenon changes both the intensity of emitted radiation and the lifetime of the luminescence. This principle is used for the measurement of e.g. oxygen by many optical measuring techniques.

7.3.2 Construction of Microoptodes

Optical fibres guide light through total internal reflection, which is caused by the difference in refraction indices between the fibre core and the cladding material. Standard fibre optical sensors are made from quartz "gradient index" fibres. Gradient index describes the fact, that the refraction index profile perpendicular to the fibre axis has a curved ("gradient") shape instead of the partially constant refraction index of step index fibres. The core of the presented fibre sensors has

a diameter of 100 µm with a 20 µm thick layer of cladding material (100/140 µm fibre). For mechanical protection, the fibre itself carries an additional polymer jacket and is inserted in a PVC tube with carbon fibres. This robust fibre cable finally has an outer diameter of 3 mm. At one end, the cable is terminated with a standard ST-plug. This allows connection to instruments as well as to other fibre cables with high precision and stability. For high spatial resolution measurements a optical fibre sensor diameter of 140 µm is too high. However, thinner fibre material has concomitant handling problems. To achieve optimum spatial resolution the fibre diameter is reduced to a diameter which is necessary for minimum invasive applications (typically < 50 µm, see part 1). This can be done either be etching of the fibre tip or by tapering in the heat of a flame. The size of the flame, the pulling force and the timing all influence the final taper geometry (Figure 7.3a). This geometry of the taper is highly important for the sensor performance and has to be optimised for each application. (A short, steep taper can compress the probe during profiling measurement. On the other hand, light

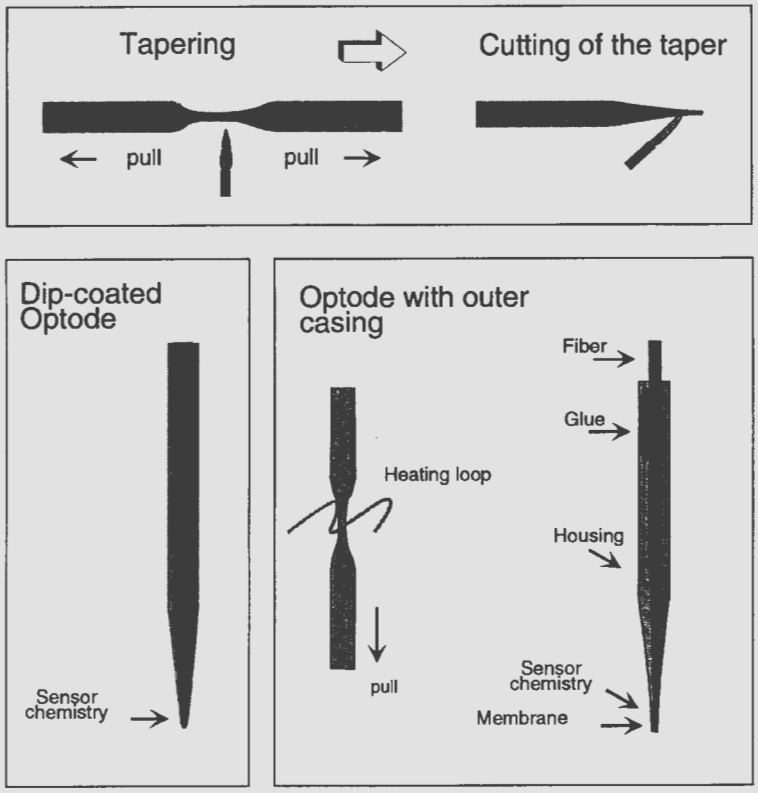

Figure 7.3 Preparation of optical microsensors: (a) tapering and cutting of optical fibre; (b) dip-coated microoptode; and (c) optode with outer casing.

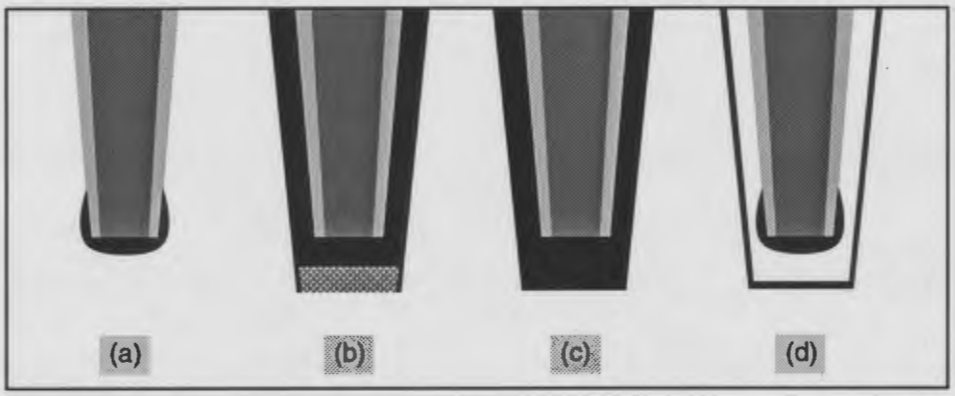

Figure 7.4 Structural overview (schematic cross sections) of microoptodes: (a) dip-coated fibre taper, various layers may be added; (b) plain fibre taper in an open microcapillary housing that is filled with indicator solution and closed with a membrane; (c) plain fibre taper in a closed microcapillary housing that is filled with indicator solution; and (d) dip-coated fibre taper in a closed microcapillary housing that is filled with a gas.

passing down to a long taper will have weak interaction and will therefore result in a small signal because of optical loss.) After tapering the fibre down to a diameter of approximately 10 μm the taper is typically cut further back at a diameter of about 30 μm. The next step in fabrication is defined by the structure and the type of sensor (Figures 7.4 and 7.18). For example, simple optical microprobes consist of tapered fibres that are aluminium coated and which have, depending on the light parameter that should be measured, scattering spheres or discs attached to the fibre tip (Figure 7.18). For microoptodes the sensing chemistry is immobilised on or around the fibre tip. From the practical point of view the easiest set-up for an optical chemical sensor is the immobilisation of the dye in or on a matrix material directly attached to the fibre tip by dip-coating. A matrix material for the immobilisation of the dye is needed which is permeable to the analyte and prevents leaching of the dye. Furthermore, the material needs to adhere well to the quartz surface and should not change the spectral characteristics of the dye. If necessary, the tip of the sensor can be over-coated by an additional layer as an optical insulation or membrane for increasing the selectivity of the sensor. For some applications the tip-coated single optical fibre is not suitable. Another approach is to surround the optical fibre by a glass casing (Figure 7.3c). The casing can be manufactured from a glass capillary by tapering it in the heat of a heating loop. For some sensors the geometry of the fibre and the casing is of high importance and has to fit well together. The control parameters for the preparation of the casing are similar to the taper process of the fibre, the size of the heated part and the pulling force.

Depending on the type of sensor the housing is closed by melting e.g. for special kind of temperature optodes (Figure 7.4c) or closed with an analyte

permeable membrane e.g. silicone for carbon dioxide optodes (Figure 7.4b). Then the tip of the housing is filled with the sensor chemistry in a liquid phase in which the tapered fibre is placed. Alternatively, the dip-coated taper can be placed in a closed casing which is a possible solution for temperature micro-optodes (Figure 7.4d).

The fixation of the optical fibre in the casing simplifies the handling of the microoptodes in experimental set-ups, which can be micromanipulators in laboratory flow chambers as well as benthic landers for *in situ* applications.

7.3.3 Oxygen Microoptode

The established type of microsensor for oxygen measurements is the Clark-type microelectrode (Revsbech, 1989). The manufacturing of this sensor is a complex and time consuming process. Normally, the Clark-type electrode exhibits a stirring sensitivity based on the electrochemical reduction of oxygen, which can be assumed as negligible for microsensors. Nevertheless, for high resolution oxygen measurements at low oxygen levels, problems can occur according to the measuring resolution of the electrodes near to their zero current.

Most of the oxygen optodes are based on luminescence quenching (Kautsky, 1939; Lübbers and Opitz, 1975). Therefore, the oxygen optode exhibits the highest signal at low oxygen concentrations. Furthermore the oxygen is not consumed and no stirring sensitivity can occur. The design of the oxygen optode is carried out as described above as sensor type A. The optode consists of a tapered optical fibre which is tip-coated with the appropriate sensing chemistry. Compared to the micro electrode production the micro optode can be prepared fast and at low costs.

As oxygen sensitive material two groups of dyes are established in literature: Ruthenium-dyes which consists of Ruthenium(II) as the central atom in the metallo-organic complex (Demas, 1976; Wolfbeis *et al.*, 1984; Lippitsch *et al.*, 1988; Klimant *et al.*, 1992; MacCraith *et al.*, 1994; Hartmann and Leiner, 1995) and Porphyrine-dyes which commonly have Platinum or Palladium as central atom in a porphyrine molecule (Wilson *et al.*, 1987; Khalil *et al.*, 1988; Papkovsky *et al.*, 1993). These dyes have excitation maxima in the blue respectively blue/green part of the spectrum and exhibit orange respectively red luminescence. Figure 7.5 shows the spectral characteristics of the molecule Tris(4,7-diphenyl-1,10-phenanthroline)-ruthenium(II) (RuDPP) dissolved in chloroform.

The compatibility of the spectral characteristics of the dyes enables the use of light emitting diodes (LED) as excitation light sources, and therefore the measurement of the luminescence intensity (or the luminescence life-time) with minimal opto-electronics (see section 3.3). The relation between the luminescence intensity I and the oxygen concentration c was first described by Stern and Volmer (1919)

$$\frac{I}{I_0} = \frac{\tau}{\tau_0} = \frac{1}{1 + K_{sv} \cdot c},$$

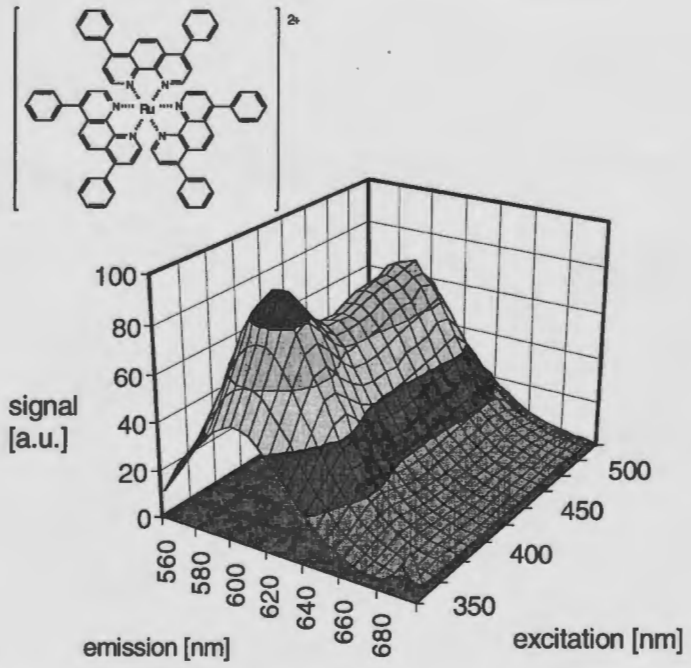

Figure 7.5 Molecular structure and excitation/emission spectra of Tris(4,7-diphenyl-1,10-phenanthroline)-ruthenium(II) solved in chloroform.

where I_0 is the luminescence in the absence of oxygen and K_{SV} the Stern-Volmer or quenching coefficient. The same equation also is valid for life-time measurements, only the intensity has to be replaced by the respective life-time parameters τ_0 and τ. In most of the real systems this relation does not sufficiently describe the measured data. Based on a two component model proposed by Carraway *et al.* (1991) the equation can be extended by a second quenchable component:

$$\frac{I}{I_0} = \frac{\tau}{\tau_0} = \frac{A}{1 + K_{sv1} \cdot c} + \frac{B}{1 + K_{sv2} \cdot c}.$$

For practical work the model has been experimentally modified with negligible error (Klimant *et al.*, 1995) by assuming one component to be non quenchable:

$$\frac{I}{I_0} = \frac{\tau}{\tau_0} = \frac{f}{1 + K_{sv} \cdot c} + (1 - f),$$

f describes the fraction of the indicator that is quenchable. The usual procedure in characterising an indicator-matrix combination is to measure calibration curves with a sufficient amount of microoptodes, made with this sensor chemistry. Then, a best fit is calculated with three variables: τ_0, K_{SV} and f. Usually we

found the fraction to be constant. Figure 7.6 demonstrates the fit of the model with the calibration data and the corresponding curve of a RuDPP indicator in an organically modified sol-gel matrix, which gave a correlation factor of $r = 0.999984$.

The choice of the dye and its immobilisation govern the sensitivity of the oxygen optodes. A high oxygen solubility leads to absolute high amounts of quenching substance at a given oxygen partial pressure. Therefore, the sensor will be very sensitive at low oxygen concentrations. A matrix material with a high oxygen solubility is silicone. Compared to silicone the oxygen solubility of polystyrene is much lower. In the last few years, sol-gel materials have became very popular, because by appropriate choice of the preparation procedure and of the precursors the permeability can be adjusted (McDonagh *et al.*, 1998). All these materials have good adhesion properties to silica (glass), which is an important prerequisite for their application as microoptodes. The oxygen sensitivity of the

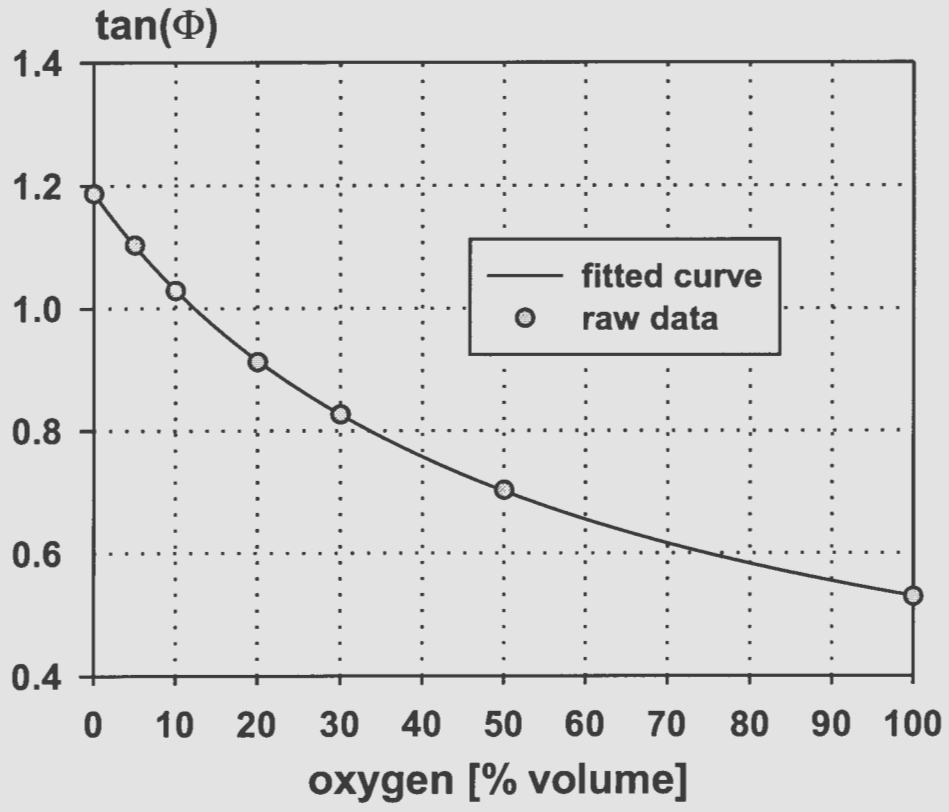

Figure 7.6 Comparison of raw measured data and the corresponding model fit for a RuDiPhe – sol-gel oxygen optode: $\Phi_0 = 49.9°$ ($\tau = 3.78\,\mu s$), KSV = 0.0184%, frac = 0.854, $f = 50\,kHz$.

indicators is a complex phenomenon. Generally, the Ruthenium-complexes are less sensitive then the Porphyrine-compounds. In Figure 7.7 normalised calibration curves for three different indicator-matrix combinations are shown. The sensitivity of each combination is optimum for a different oxygen concentration range (Figure 7.7, see legend box), which demonstrates the ability to tune the oxygen microoptode for the corresponding application. Optodes with very high sensitivity in the low oxygen range (Figure 7.7, 0–10%) as well as sensors with nearly homogeneous sensitivity over the whole range (Figure 7.7, 0–800%) can be prepared.

Typically, the oxygen microoptode is a type A sensor (Figure 7.4a) (tapered fibre and tip-coated sensor chemistry). The thin sensing layer usually does not absorb all the excitation light. Therefore, a certain amount of light may leave the sensor at its tip – which can cause problems in photosynthetic environments, because the excitation light for the dye changes the local light conditions for the

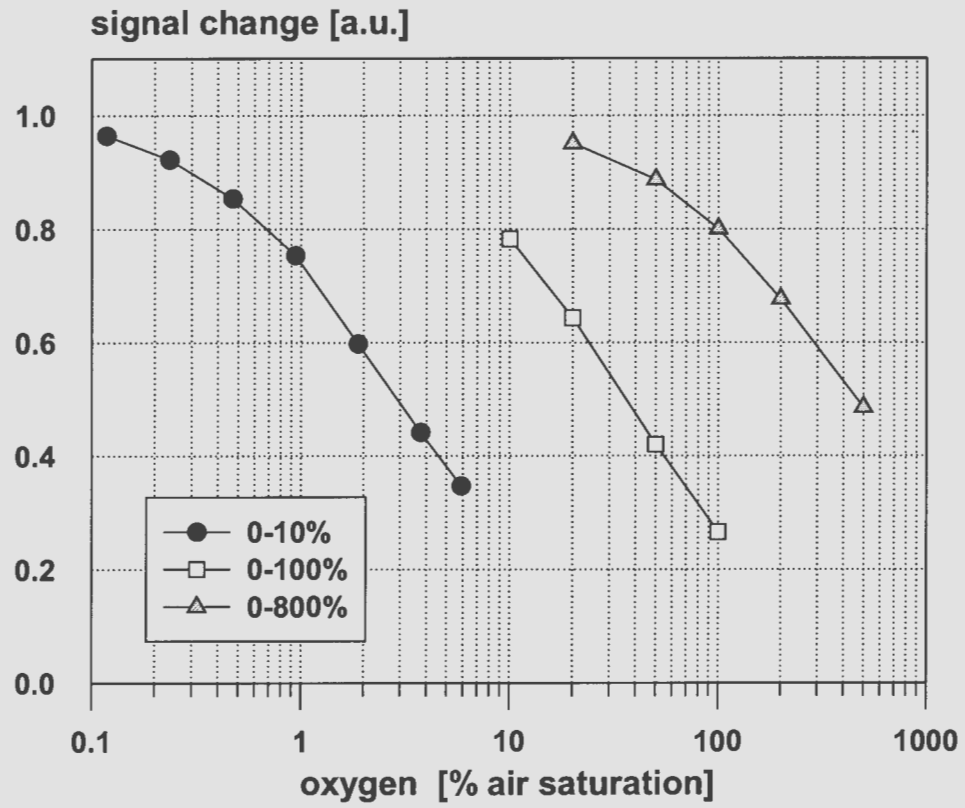

Figure 7.7 Comparison of calibration curves of oxygen microoptode optimised for different oxygen measuring ranges (see legend box). The oxygen zero point of all curves is suppressed because of the logarithmic scale.

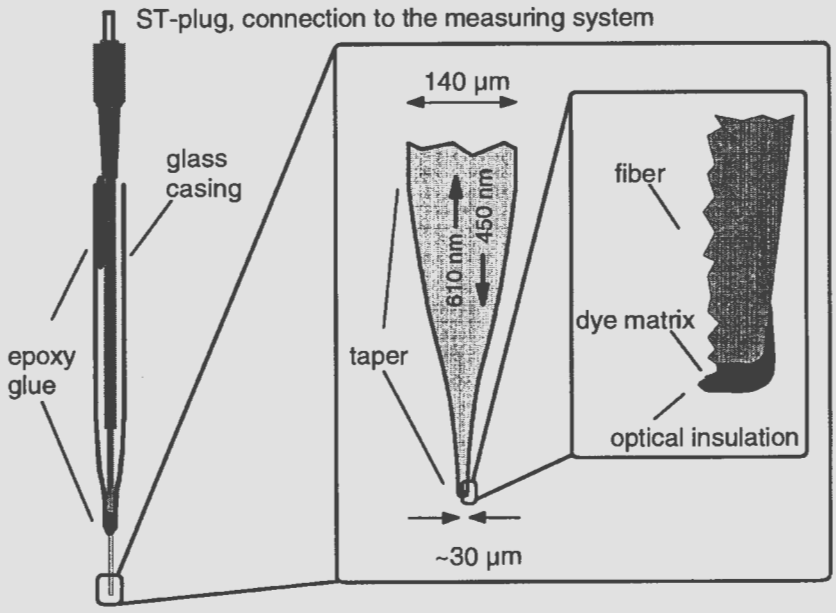

Figure 7.8 Schematic drawing of an oxygen microoptode for application in benthic landers.

microorganisms and might induce photosynthesis. This problem can be solved by an additional layer on the sensor tip which prevents the light from leaving the sensor. This layer is called optical insulation and usually is made of a highly oxygen permeable material like carbon black silicone. In Figure 7.8 an oxygen microoptode consisting of an additional casing for better handling and optical insulation is shown in detail.

The oxygen microoptode was successfully applied in laboratory set-ups, as can be seen in Figure 7.9. An oxygen microoptode and an oxygen microelectrode were combined to form a double tip sensor with an approximate distance of 100 µm between the tips. With the combined sensor depth profiles of oxygen were measured in a dense microbial mat from a hypersaline lake (Solar Lake, Egypt). The mat was kept in a steady flow, at constant salinity and temperature in a flow chamber. The results obtained with illumination and darkness illustrate nicely the equivalence of both microsensors. The negligible differences in the curves are due to the natural heterogeneity of the mat and the spatial distance between the tips. Furthermore, oxygen microoptodes have been applied on lander systems (Glud *et al.*, 1997). Test and characterisation measurements exhibited a low (for practical work, negligible) pressure influence on the sensing chemistry and the sensor signal up to 600 atm (Kohls *et al.*, 1996–1998, unpublished results). Therefore, oxygen measurements in the deep sea on lander systems are entirely feasible, as demonstrated by Wenzhöfer *et al.* (1998).

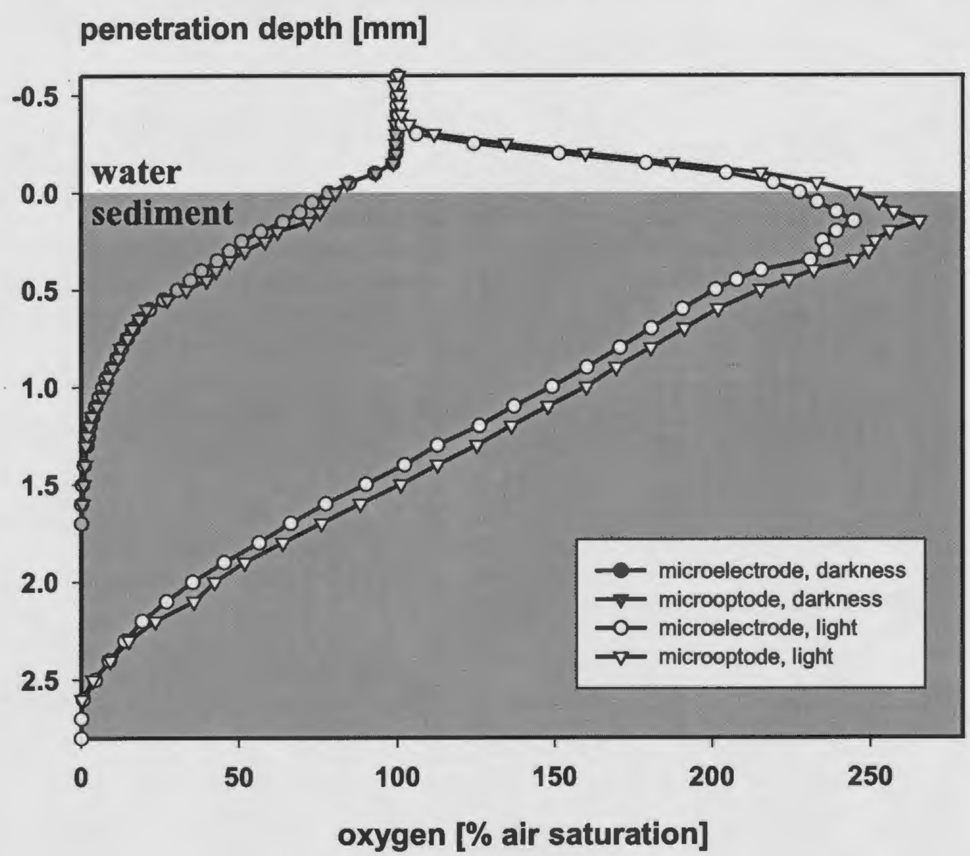

Figure 7.9 Oxygen depth profiles of a microsensor combination made of an oxygen microoptode and an oxygen microelectrode measured in a microbial mat from a hypersaline lake (Solar Lake, Egypt) in light and darkness conditions (see legend box). The distance between the two microsensor tips was approximately 100 µm.

7.3.4 pH Microoptode

A broad range of pH sensitive dyes is described in the literature (Bishop, 1972; Munkholm *et al.*, 1986; Lübbers *et al.*, 1977; Leiner, 1991, and reviewed in Wolfbeis, 1991). For the analytical pH range of seawater, pH 7 to 9 the number of useful dyes is limited. An optical pH measurement usually can determine pH to a very high accuracy over a dynamic range of ± 2 pH units of the pK value of the dye (The pK value is the – log of the equilibrium constant K from the reaction of the dye with the proton). Therefore the pK of the immobilised dye has to be in the seawater range. The applicable dyes exhibit different spectral characteristics in their protonated and deprotonated form, based on the pH of

the surrounding/medium. Most of the dyes have more than one acidic proton and corresponding pK values and sensitivity ranges.

$$H_nI \xleftarrow{K_1} H^+_{n-1} + I^{1-} \xleftarrow{K_2} 2 \cdot H^+_{n-2} + I^{2-} \xleftarrow{K_3} \wedge .$$

Over the relatively small pH range of the marine environment usually just one pK is used for measurement. The constant K for a single equilibrium is expressed by

$$K = \frac{[H^+] \cdot [I^-]}{[HI]},$$

where it has to kept in mind that the equilibrium constant refers to the activity of the species. If the activity coefficient f is taken into account, the relation between the dye forms and the pH value can be expressed by the Henderson-Hasselbalch equation:

$$pH = pK + \log\left(\frac{[I^-]}{[HI]}\right) + \log\left(\frac{f_{I-}}{f_{HI}}\right)$$

Absorption dyes useful for application at marine pH values are e.g. sulphophthalein indicators like thymol blue, m-cresol purple, cresol red or phenol red (Robert-Baldo *et al.*, 1986). Furthermore a number of luminescence dyes are known, such as hydroxypyrenetrisulfonicacid (Leiner, 1991) or different rhodamin and fluorescein derivates like SNARF and SNAFL dyes (Molecular Probes Inc.). The most common technique in optical pH determination is based on intensity measurement because the lifetime of pH sensitive luminescence dyes is rather short (range of ns). A set-up for optical pH measurements using lifetime evaluations would be much more complex and expensive than electrochemical methods and, therefore, offer no real alternative to existing microelectrodes at the moment.

The most critical point for all kinds of optical pH measurement is the immobilisation of the dye. In order to reach a high solubility for protons, it is necessary to immobilise the dye in or at a hydrophilic material such as cellulose derivatives or sol-gels. Due to the fact, that pH dyes are polar substances they are usually soluble in water. This enables the leaching of the dyes from their matrix. Therefore the dyes have to be bound covalently or at least absorbed at a material which has a higher affinity to the dyes than water. The absorption dye N9 (Merck) can bound covalently on a prepared cellulose acetate material. In Figure 7.10 the pH dependent absorption of the dye is shown. Detailed characterisation of the pH dependent absorption of the dye identifies the optimum pH sensitive regions (450 nm and 590 nm). Wavelengths at 480 nm and >800 nm do not exhibit a distinct pH dependence and can thus be used for referencing purposes (e.g. correction of fibre bending effects and other pH-independent changes in light intensity).

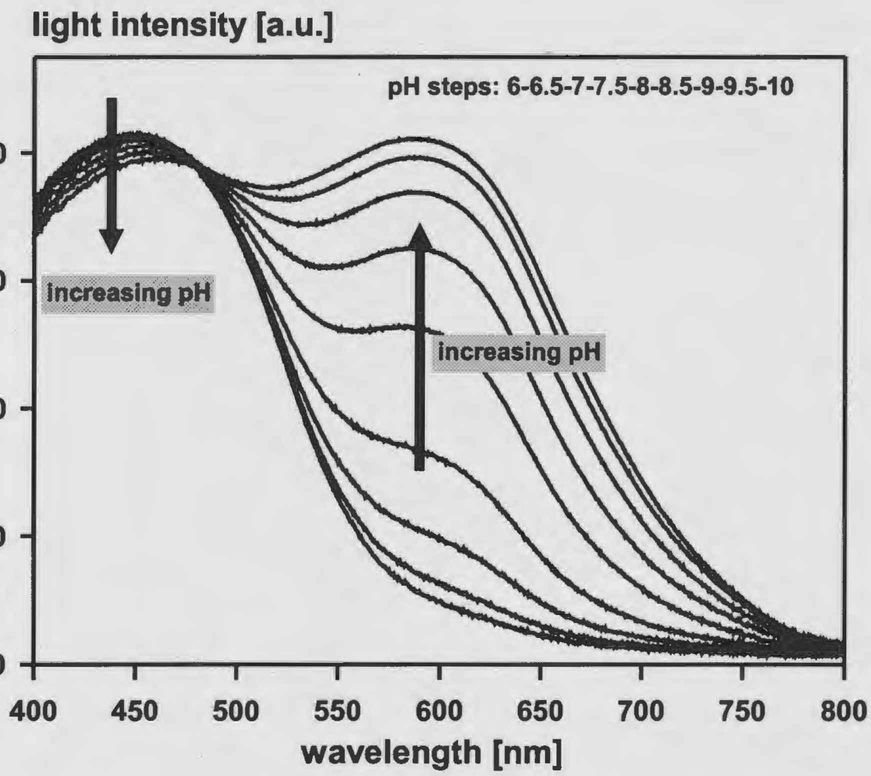

Figure 7.10 pH dependent absorption spectra of the indicator N9. The arrows indicate the direction of change of each spectrum when the pH is increased. The isosbestic point is at 480 nm.

In practice, the amount of reflected and backscattered light from the indicator at the fibre tip is monitored via an optoelectronical set-up, where blue and yellow LEDs are used as light sources and a photodiode for detection. By using yellow light for monitoring the 590 nm region this dye exhibits an apparent pK around the natural pH of seawater, i.e. at pH 8.2 (Figure 7.11). The pH microoptode with a tip diameter smaller then 40 μm allows pH measurements at an approximate accuracy of ± 0.05 pH units over a range of pH 7–9. First pH depth profiles (Kohls *et al.*, 1997) in a coastal sediment resulted in pH microprofiles similar to the depth profiles that have been observed with pH microelectrodes (Revsbech *et al.*, 1983).

7.3.5 Carbon dioxide Microoptode

CO_2 in the gas phase can be measured directly by infrared absorption. This is the most exact way to determine CO_2 with negligible cross sensitivity. For practical

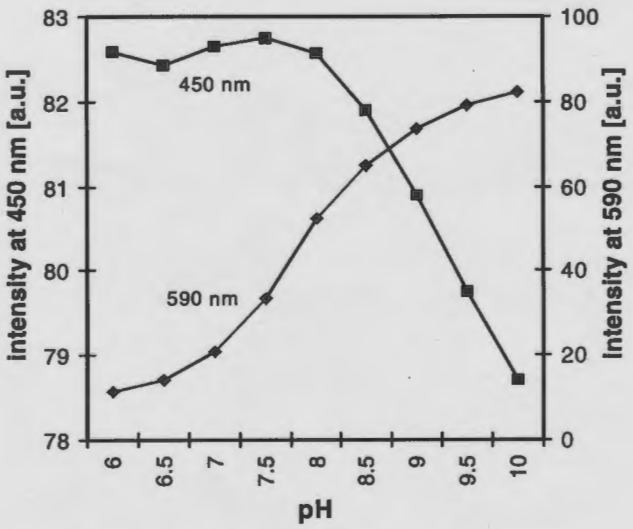

Figure 7.11 Calibration curves of the pH microoptode (N9), measured light intensity vs. pH units, with blue (squares) and yellow (diamonds) illumination light.

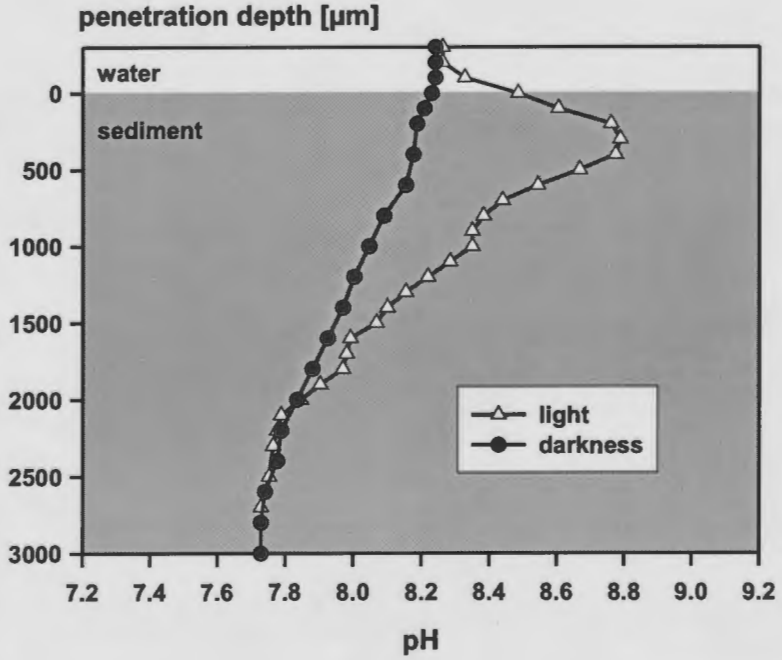

Figure 7.12 pH depth profiles, obtained with an absorption based (N9) pH microoptode, measured in a North Sea sediment in light and darkness conditions (see legend box).

microsensor applications this technique is not useful. Other techniques are based on the Severinghaus-principle (Severinghaus and Bradley, 1958; Lübbers and Opitz, 1975; Munkholm *et al.*, 1988; Leiner, 1991). Here CO_2 diffuses through a gas-permeable membrane into a buffer reservoir, where the induced shift in pH is monitored with a pH sensor. This can be easily realised with optical microsensors. The sensor, type B, consists of an outer glass-microcapillary, which is sealed with a thin silicone membrane and filled with a solution of an appropriate dye. The dye must have its pK value at the pK of the equilibrium between hydrogencarbonate and carbonate,

$$CO_2 + H_2O \xleftarrow{K_1} HCO_3^- + H^+ \xleftarrow{K_2} CO_3^{2-} + 2 \cdot H^+$$

A useful dye for this purpose is e.g. hydroxypyrenetrisulfonicacid (HPTS, Leiner, 1991). HPTS is a pH sensitive luminescence dye with a high quantum yield and an apparent pK value of 7.5. The absorption/emission spectrum and molecule structure of HPTS is shown in Figure 7.13. HPTS exhibits an excitation maximum at 455 nm (compatible to blue LEDs) and an emission at 515 nm. The

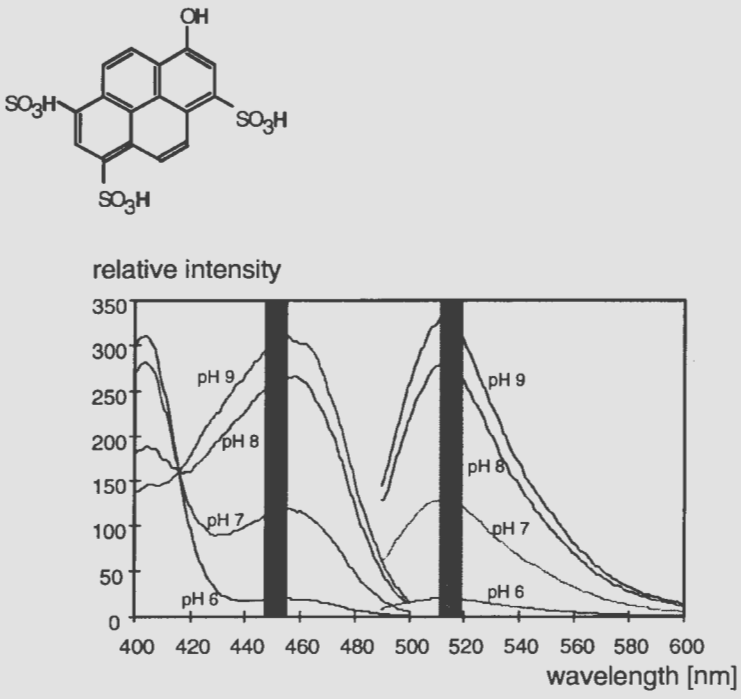

Figure 7.13 Molecular structure and excitation/emission spectra of hydroxypyrenetrisulfonicacid (HPTS) at different pH values. The marked areas indicate the optimum wavelengths for excitation (black) and emission (grey).

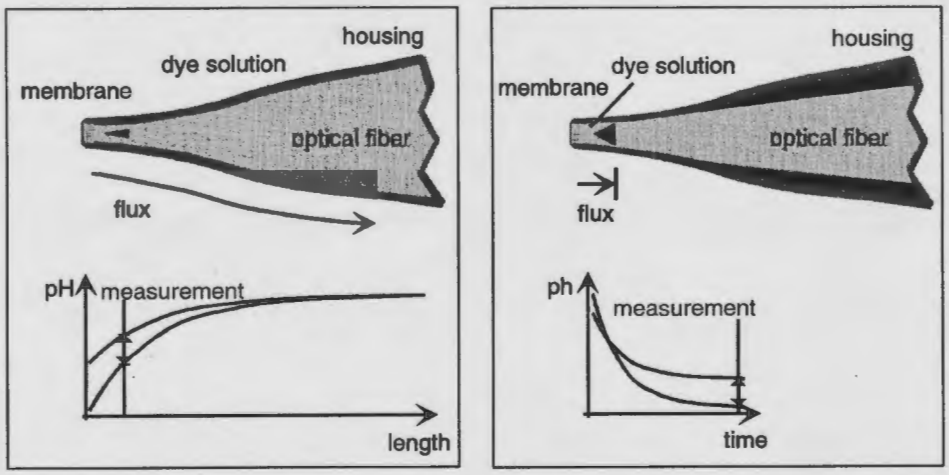

Figure 7.14 Structural pathways for CO_2 microoptodes with (a) a dynamic variation and (b) a static variation of the Severinghaus-principle.

Stokes-Shift of about 60 nm enables a pH sensitive luminescence intensity measurement.

Two pathways using the Severinghaus principle are possible in microscale: Figure 7.14(a) shows a dynamic measuring principle, where an efficient diffusive exchange from the tip environment to a larger buffer reservoir occurs, and Figure 7.14(b) shows a static measuring principle with a semi-closed buffer reservoir in the sensor tip (Kohls and Epping, 1997, unpublished results). The performance of the optode can be "tuned" by the internal dye concentration and the buffering capacity. High dye and buffer concentrations give a high sensor signal and high detection limits. For measurements in the marine environment high CO_2 sensitivity is required (seawater contains 10–15 µM dissolved CO_2). By using the static type CO_2 optode a sufficient sensitivity with a detection limit < 5 µM CO_2 has been demonstrated (Figure 7.15). The response time of a CO_2 microoptode with a tip diameter below 40 µm is less than 2 minutes – which is fast for a CO_2 sensor but somehow slower than other microoptodes.

7.3.6 Temperature Microoptode

Both respiration and photosynthesis of microorganisms are strongly effected by changes in temperature. The determination of the temperature distribution in sediments and microbial mats is therefore of importance to better understand the regulation of these metabolic processes. Furthermore, if chemical parameters are measured with microsensors, the presence of temperature gradients would cause errors in the measurement due to the lack of temperature compensation of the measuring signal. Obviously, there is interest in microsensors which allow the

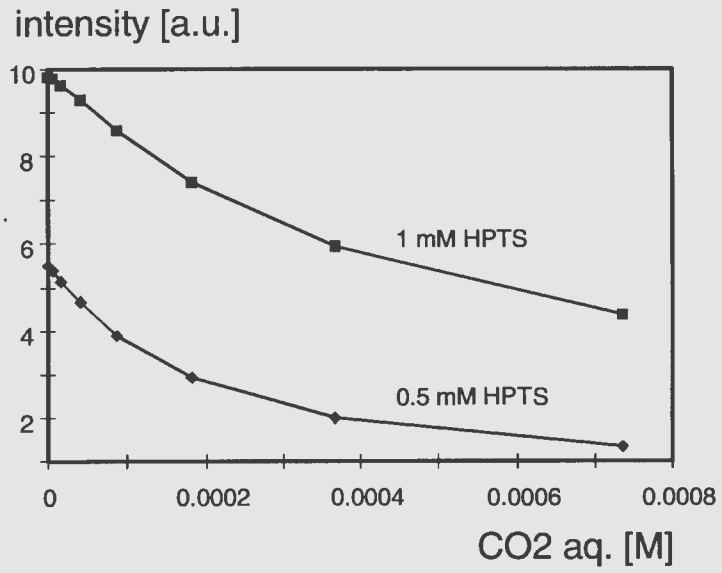

Figure 7.15 Calibration curves for the CO_2 microoptode with high (squares) and low (diamonds) dye-concentration/buffering capacity.

measurement of temperature to the same spatial resolution as chemical microsensors. A potential strategy for the design of temperature microoptodes is the measurement of the temperature dependent luminescence of luminophores with long decay times. The excited state of certain luminophores is thermally deactivated, resulting in a correlation between temperature and luminescence lifetime. Certain solid materials (such as Cr^{3+}-doped crystalline materials) or transition metal complexes are potentially useful for optical temperature sensing (Zhang *et al.*, 1993; Alcala *et al.*, 1995; Grattan and Zhang, 1995). Demas and De Graff (1992) suggested to use luminescent ruthenium(II)-complexes as temperature indicators because they exhibit a strong temperature dependence of the quantum yield and the luminescent lifetime. Recently new temperature microoptodes based on this concept were presented (Holst *et al.*, 1997; Klimant *et al.*, 1997). The ruthenium(II)-tris-1,10-phenanthro line complex ($Ru[phen]_3$) was selected as most promising indicator for designing new temperature microoptodes, since its luminescence lifetime is strongly effected by temperature in the relevant range between 0 and 50 °C (appr. 2.5%/°C). Three different concepts to design temperature microoptodes were realised, which correspond to the microoptode types that are shown in Figure 7.4(a), (c) and (d).

The design of sensor type A (Figure 7.4) is identical to the described oxygen microoptodes and is based on tapered optical fibres which are dip-coated with a thin temperature sensitive film. The sensing film contains the $Ru[phen]_3$-complex (Figure 7.16, ind 1) embedded in a matrix which has a negligible or

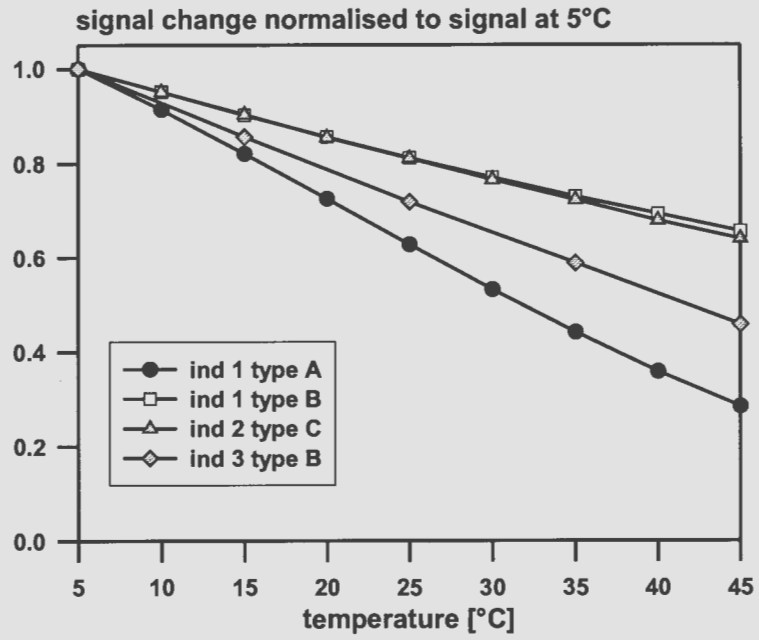

Figure 7.16 Temperature calibration curves of 4 different temperature microoptodes (see legend box and text for explanation) in the range of 5–45 °C. The signal of each sensor has been normalised to the value at 5 °C.

even zero cross sensitivity towards oxygen. The most favourable matrices for immobilisation are PVC and sol-gel glasses with a very low oxygen permeability. Microoptodes of type [a] (Figure 7.4) allow the miniaturisation down to 10 µm by using the preparation process for dip-coated microoptodes (see section 2.2.1). Unfortunately the ruthenium complex embedded in a solid matrix (Figure 7.16, and ind 1 type [a]), shows a temperature coefficient that is a factor of 2–3x lower compared to the aqueous solution (Figure 7.16, ind 1 type [c]). The advantage of type [a] sensors (Figure 7.4) are their very simple preparation.

The type [c] sensor (Figure 7.4) consists of a tapered and sealed glass capillary, which is filled with a deaerated solution of the temperature indicator (Figure 7.16, ind 1 type [c]). A tapered optical fibre is then introduced into the tip of the glass capillary to measure the luminescence lifetime (Figure 7.4c) in the small volume that is illuminated by the fibre tip. The internal solution contains $Ru[phen]_3$ (Figure 7.16, ind 1) and an excess of sodium dodecylsulfate or polystyrene sulfonic acid to enhance the luminescence lifetime and the signal intensity. Sodium sulphite was added as oxygen scavenger because oxygen is (as described in section 2.2.2) an efficient quencher of luminescence. The outstanding feature of this microoptode is its very high temperature coefficient which makes it suitable for high resolution temperature sensing (Figure 7.16, ind 1 type [c], 7.17).

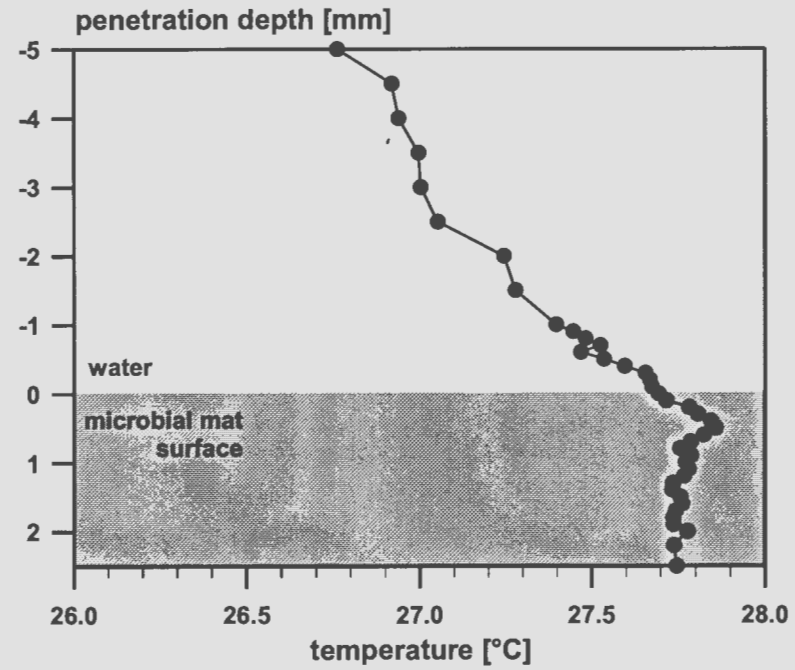

Figure 7.17 Temperature depth profile measured with a temperature microoptode type [c] in a microbial mat from a hypersaline lake (Solar Lake, Egypt) under light condition.

Type [d] sensors (Figure 7.4) use the cross sensitivity of temperature on the response of an oxygen microoptode. The sensor consists of an oxygen microoptode which is located in a sealed glass capillary which is filled with air. Therefore, the oxygen partial pressure is kept constant during the measurement. Temperature has two well-known effects on the sensor response. First, the excited state of the luminescence indicator is thermally deactivated, resulting in a decrease of the luminescence lifetime with increasing temperature. Second, an increase in temperature results in an increase of the quenching efficiency and therefore decreases of the luminescence lifetime. This is caused by the increase in oxygen permeability of the polymer with increasing temperature. Type [d] sensors (Figure 7.4) allow the use of luminescence indicators having longer lifetimes since, due to the constant oxygen concentration, the oxygen does not need to be excluded. Therefore, phosphorescent platinum(II)-porphyrins (Figure 7.16, ind 3 type [d]) which have luminescence lifetimes in range up to 100 µs have been selected as suitable.

Sensors of type [a] (Figure 7.4) show the fastest temperature response (a few milliseconds) allowing real time measurements. Type [d] sensors (Figure 7.4) exhibit the slowest response since there is a kinetic limitation to the exchange of oxygen between the sensing layer and the gas phase with changing temperature.

Therefore, the response is limited by the response towards oxygen, which is in the order of 100 ms up to a few seconds, depending on the immobilisation matrix used and the thickness of the sensing layer. Since the luminescence lifetimes of the temperature microsensors are in the same order of magnitude than these of oxygen microoptodes, the same instrumentation may be used. An example of a measured temperature gradient in a dense light absorbing microbial mat with a temperature microsensor of type [c] is given in Figure 7.17. A significant increase of temperature in the biological system was observed during illumination with the visible light of a halogen lamp.

7.4 OPTICAL MICROPROBES

While fibre-microsensors for physico-chemical variables (microoptodes) rely on reversible changes of an optical indicator immobilised at the tapered tip of an optical fibre, optical microprobes transmit the optical information from the surroundings of the optical fibre tip direct to the detector. Spectra can be acquired by coupling the microprobe fibre to a spectrum analyser, i.e. a spectrograph coupled to diode arrays and CCD's (e.g. Kühl and Jørgensen, 1992) or, alternatively, a scanning monochromator coupled to a photomultiplier or photodiode (e.g. Vogelmann and Björn, 1984; Garcia-Pichel, 1995; Jørgensen and Des Marais, 1986). Specific spectral information within a given wavelength region, e.g. the light available for photosynthesis (400–700 nm), can be obtained by connecting the microprobe to a photomultiplier or a photodiode, where the detector response has been modified with band pass and/or colour compensation filters (Kühl *et al.*, 1997). The actual spectral range depends on the characteristics of the light detector system and on the optical properties of the fibre material. Currently, microprobes and measuring systems are available for light measurements from UV to NIR.

The following section describes fibre-optic microprobes for light measurements in studies of photosynthesis and sediments. More details about definitions, construction of microprobes and their application can be found elsewhere (Kühl and Jørgensen, 1994; Kühl *et al.*, 1994a).

7.4.1 Field Radiance Microprobe

The first fibre-optic microprobes were developed for measuring the radiation flux incident from a specific direction and solid angle in biofilms and sediments (Jørgensen and Des Marais, 1986) as well as in leafs (Vogelman and Björn, 1984). This parameter is the field radiance, which is the fundamental optical parameter for describing light fields. Field radiance microprobes can easily be made from a single strand optical fibre with a flat cut light collecting end, which can be tapered down to even sub-micron diameters (Figure 7.18). In most practical applications in aquatic environments, microprobes with 10–50 μm tip diameter are used. For

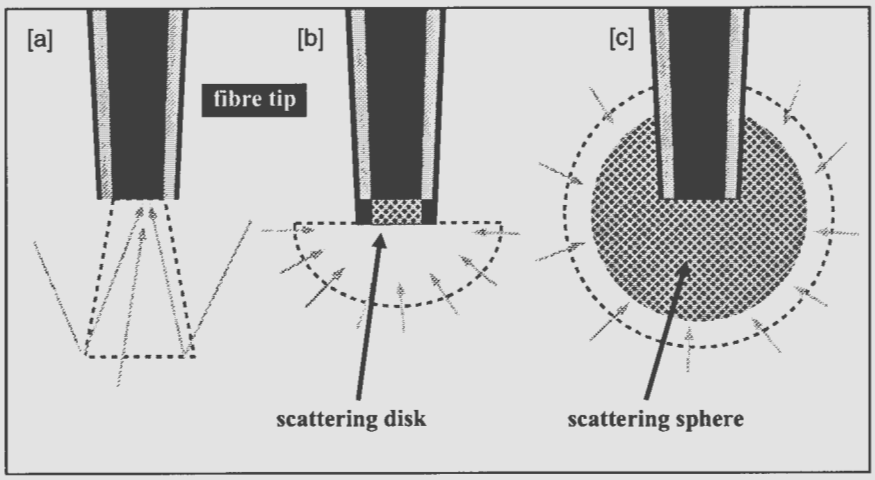

Figure 7.18 Schematic cross sectional overview on different microprobes: [A] radiance microprobe and sensor for surface detection; [B] irradiance with attached scattering microdisk; and [C] scalar irradiance microprobe with attached scattering microsphere. For radiance and irradiance measurements the fibre tips are Aluminium coated.

microscale light measurements, it is important to coat the tapered sides of the fibre tip with a metal film or some enamel paint in order to avoid light leakage into the fibre via the taper.

Field radiance microprobes can be used for high spatial resolution measurements of radiance spectra in sediments and biofilms (Kühl and Jørgensen, 1992). This enables studies of the zonations of differently pigmented phototrophs often found in these systems. It is also possible to monitor the migration of phototrophs by such measurements, e.g. by following the change in spectral composition of backscattered and reflected radiance (Kühl *et al.*, 1994a). Furthermore, by measuring depth profiles of field radiance at different angles relative to the incident light, it is possible to separate collimated and scattered light fluxes in sediments and biofilms (Figure 7.20). From such measurements of angular radiance distribution it is possible, after some mathematical treatment of the measured data (Kühl and Jørgensen, 1994; Fukshansky-Kazarinova *et al.*, 1997, 1998), to extract information of the inherent optical properties of the investigated sediment or biofilm. Thus, detailed information about light fields and optical properties of sediments and biofilms can be gained from the extensive application of field radiance microprobes.

The most recent application of field radiance microprobes involves microscale measurements of fluorescence. For such measurements, the microprobe is connected to the excitation source and the detector via a similar set-up as used for microoptodes (see Figure 7.26). By appropriate choice of excitation wavelength, excitation and emission filters, it is possible to monitor the microscale distribution

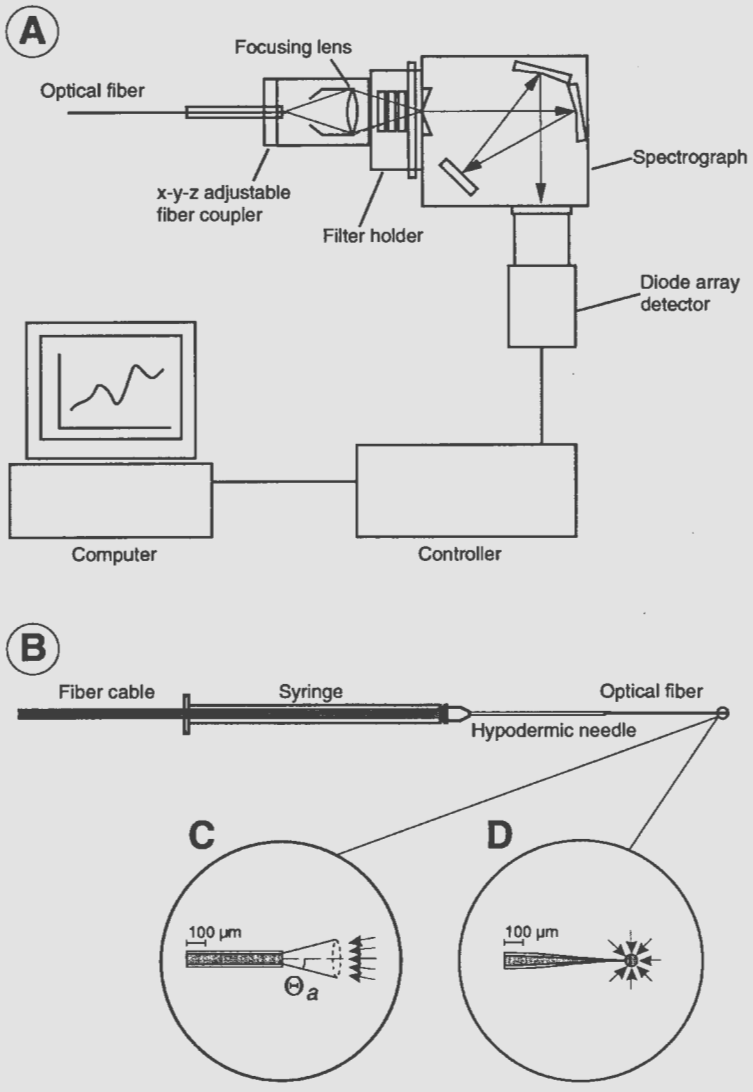

Figure 7.19 Example of optoelectronical set-up for fibre-optic microprobes and types of microprobes: A. Intensified diode array detector system; B. Basic design of a fibre-optic microprobe; C. Tip of microprobe for measuring field radiance. The fibre tip can also be tapered to smaller diameters; and D. Spherical tip of a microprobe for measuring scalar irradiance (from Kühl and Jørgensen, 1992).

of photopigments, such as chlorophyll *a*, in sediments and biofilms (M. Kühl unpublished results). Furthermore, by applying a more sophisticated measuring system, it is possible to measure photosynthetic electron transport via fluorescence measurements with a radiance microprobe (Schreiber *et al.*, 1996).

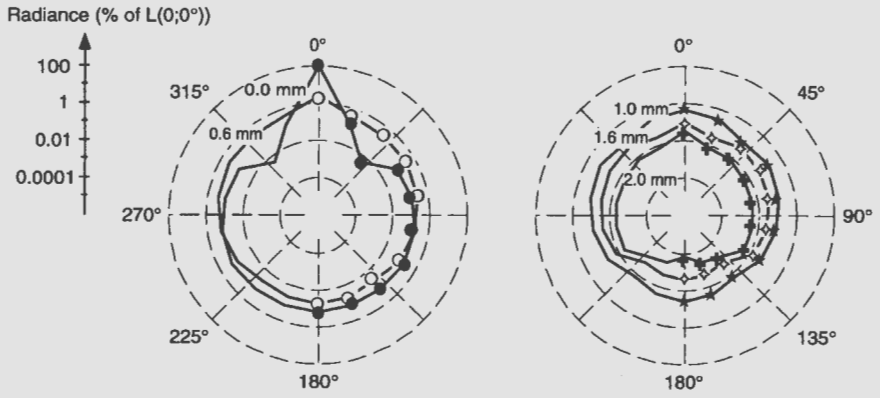

Figure 7.20 Angular radiance distributions of 650 nm light measured with a fibre-optic microprobe in a coastal sediment. Numbers on curves indicate depth below the sediment surface. Symbols indicate measured values expressed on a log-scale in % of the vertically incident radiance (0°) at the sediment surface. From such data sets, the optical properties of sediments can be calculated (from Kühl *et al.*, 1994a).

7.4.2 Irradiance and Scalar Irradiance Microprobe

While detailed information about the light field in sediments and biofilms can be gained from numerous measurements with field radiance microprobes, they are not applicable for routine measurements of total available light for e.g. photosynthesis. Sediments and biofilms are strongly scattering and absorbing systems, where the photosynthetic microbes live in a diffuse light field (Figure 7.20) and receive significant amounts of light from all directions around them. Measurements with radiance microprobes in a certain direction, therefore, only collect a fraction of the available light. The total light flux from all directions can be estimated by integration of angular radiance distribution data. This is very time consuming and not easily applicable to photosynthesis studies of sediments and biofilms. Alternatively, the light collecting properties of the optical fibre tip can be modified to integrate the radiant flux over certain directions (Figure 7.18).

The integral of field radiance incident on a horizontal plane from an upper or lower hemisphere is called the downwelling and upwelling irradiance, respectively. A microprobe for irradiance can be manufactured by fixing a small disk of light scattering material at the end of a tapered fibre, and such a microprobe acts as an almost ideal cosine collector, i.e. an ideal irradiance meter (Lassen *et al.*, 1994; Kühl *et al.*, 1994b).

Irradiance is a common measure of light intensity and is often used for estimating light availability in the aquatic sciences. However, in turbid waters and especially in sediments, biofilms, plant and animal tissue and other optically dense media irradiance measurements are not appropriate for quantifying the

total available light. A better measure is the integral of radiance from all directions about a point, i.e. the scalar irradiance. The scalar irradiance is the most relevant light field parameter for measuring total light availability in scattering.

Scalar irradiance microprobes can be made by immobilising a small light scattering sphere (70–150 µm diameter) at the tapered end of an optical fibre (Figure 7.18). The sphere efficiently scatters incident light, and this leads to the same probability for incident photons (irrespective of their angle of incidence) to be channelled into the fibre tip and, subsequently, to the detector. A microprobe with such an isotropic light collection thus measures scalar irradiance. The sphere can either be formed by dip coating of the fibre tip in a TiO_2-doped methacrylate (Lassen *et al.*, 1992) or by forming a vitro-ceramic sphere by careful heating of a fibre tip, which is drawn to a thin filament and dipped in MgO (Garcia-Pichel, 1995).

Scalar irradiance microprobes can be used to obtain information about the microscale light availability in photosynthetic sediments and biofilms, e.g. by measurements of attenuation spectra (Figure 7.21) and depth profiles of light penetration (Figure 7.22b). Such measurements can then be combined with

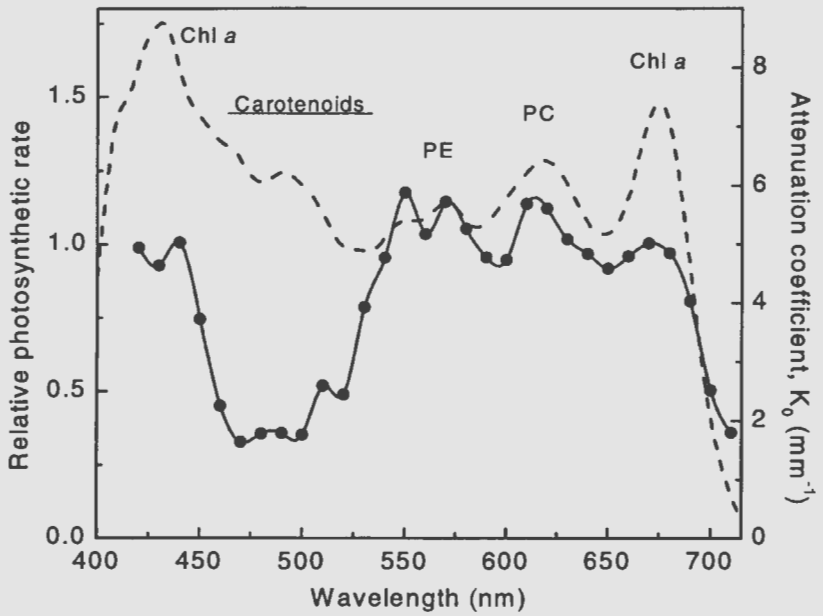

Figure 7.21 Attenuation spectrum of scalar irradiance (dashed curve) measured with a fibre-optic microprobe over the the upper 0.1 mm of a photosynthetic biofilm. Scalar irradiance measurements were also combined with measurements of photosynthesis with an oxygen microsensor to measure the action spectrum of photosynthesis. Absorption regions of Chorophyll *a*, carotenoids, and phycobiliproteins (phycocyanin, PC, and phycoerythrin, PE) are indicated on the Figure (from Kühl *et al.*, 1996).

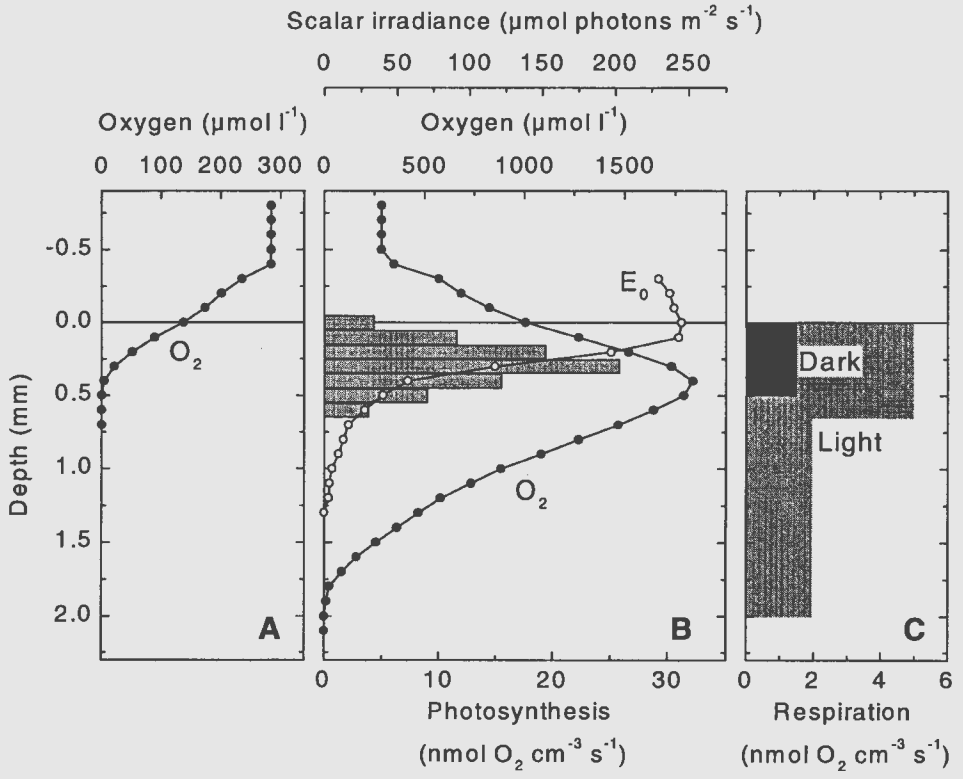

Figure 7.22 Oxygen, photosynthesis and 400–700 nm light penetration measured with microsensors for oxygen and scalar irradiance in a photosynthetic biofilm: A. In the dark, oxygen only penetrates 0.5 mm; B. In the light, photosynthesis (indicated with bars in the graph) leads to supersaturation of the biofilm with oxygen. Photosynthesis is confined to the upper 0.5 mm of the biofilm due to strong attenuation of scalar irradiance, E_0, by the densely populated biofilm; and C. Calculated respiration rates within the biofilm in dark and light. The respiration is stimulated in the light.

microsensor measurements of photosynthesis and chemical variables to obtain information about the light regulation of photosynthesis and respiration in sediments and biofilms (Figures 7.21, 7.22; Kühl *et al.*, 1996; 1997; Garcia-Pichel and Bebout, 1996).

7.4.3 Microprobe for Surface Detection

An important prerequisite for obtaining useful information from microsensor measurements (e.g. calculation of diffusive boundary layer thickness, reaction rates and fluxes), is the ability to determine the exact position of the sensor tip relative to the interface between the biogeochemical system and the overlying

water (i.e. the water-sediment interface). In the laboratory, penetration of the sensor tip into a sediment or biofilm is often determined visually using for instance a dissection microscope. However, visual inspection can be imprecise or even false – especially if the surface is characterised by a high level of heterogeneity or the overlying water layer is turbid. During *in-situ* application of microsensors visual determination of the surface is generally impossible and is usually estimated from measurements with relatively large resistivity probes (Andrews and Bennett, 1981; Tengberg *et al.*, 1995).

Reflection based optical methods for surface detection and positioning control have found many industrial applications (Dakin and Culshaw, 1988). Such sensors illuminate an object surface and measure the level of reflected and backscattered light via the same optical fibre.

Recently, this method was adapted in the design of a very simple optical measuring system for detecting the sediment-water interface with a high spatial resolution by use of a simple fiber-optic microprobe (Klimant *et al.*, 1998). The microprobe is a tapered optical fibre with a tip diameter of 20–40 µm, terminated with a standard ST-fibre connector. The optical system is a simplified version of a set-up developed for optical oxygen microsensors (Figure 7.28, Figure 7.26). A NIR laserdiode was selected as light source ($\lambda = 780$ nm), since at this wavelength the intrinsic light absorption of sediments is low and no stimulation of photosynthesis occurs. The laser light was frequency-modulated to separate the signal from ambient light. Due to the efficient coupling of the laser diode light into the fibre, a simple photodiode was used to measure the reflected light with a sufficient signal-to-noise-ratio. A 2×2 fibre coupler (see section 3.1) was used to minimise contributions from reflected light generated in the optical system.

The operating principle of the surface detection system is simple. When the microprobe tip is moved towards the water-sediment interface (Figure 7.23, [a]–[c]), an increasing amount of backscattered and reflected light from the sediment surface is captured by the fibre (Figure 7.23, smaller black arrows). The highest relative signal change occurs, when the fibre tip reaches the water-sediment interface (Figures 7.24, 7.25) causing a significant shift in the scattering properties.

The spatial resolution of the surface detection is related to the diameter of the fibre tip. The precision of the measurement increases with decreasing sensor size. With a 20 µm sensor the surface of a highly scattering surface may be determined with a resolution better than 50 µm (Figure 7.24). It is significant that miniaturisation not only improves the spatial resolution of the measurement but also results in a strong increase of the signal intensity. The shape of the sensor response curve not only depends on the sensor geometry but also on the optical properties of the sediment surface itself, i.e. refractive index, size and shape of the sediment particles. Best results were obtained in fine or silty sediments, whereas the use of the surface detection sensors in sandy sediments with larger grains (< 100 µm) was complicated (Klimant *et al.*, 1998).

The surface detection system can be combined with other microsensors, simply by fixing the tapered fibre to a microelectrode or microoptode. Figure 7.25

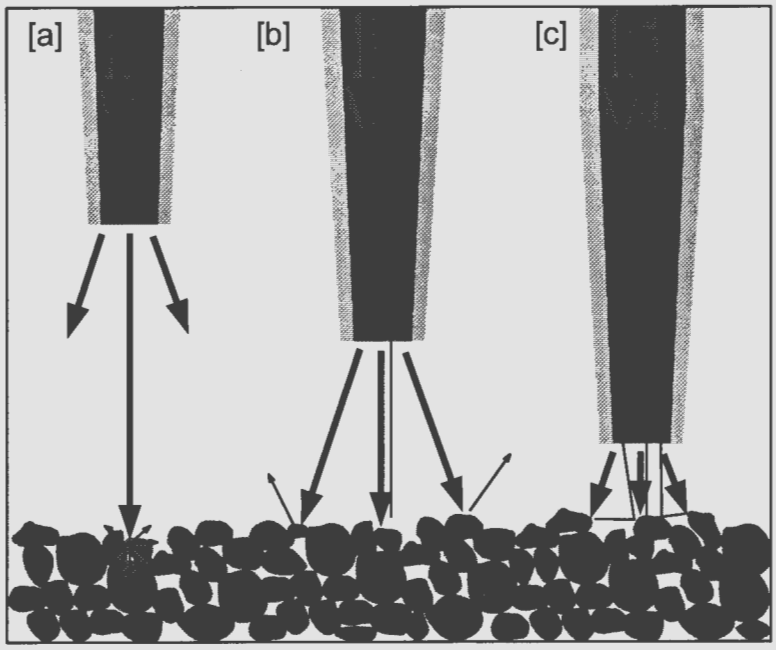

Figure 7.23 Principle of sediment surface detection (schematic drawing): (a) The NIR light (downward pointing black arrows) emitting fibre taper is far away from the surface, the light that reaches the surface is reflected and scattered (biggest part is forward scattered) by the sand grains of the sediment surface, but now light is captured by the microsensor; (b) The fibre tip approaches the surface and first amounts of the reflected and backscattered light from the surface are captured by the fibre (upward pointing black arrows); and (c) The fibre is near to touch the surface, before the amount of reflected and backscattered light depends on single grains and the pore space more light is captured by the sensor tip (thicker upward pointing black arrows, compared to b).

shows the respective depth profiles measured with such a combined sensor in a sandy North Sea sediment. The results show a good correspondence of the optically determined surface position and the surface position one would infer from the oxygen measurements.

An important field of application, which can be envisioned for the surface detection system in combination with microsensors, is for *in situ* measurements with benthic profiling landers, where visual inspection of surface penetration is not possible.

7.5 SUBMICRON OR NANO SENSORS

The smallest fibre optical chemical sensors (so-called sub-micron or nanooptodes) were developed by Tan *et al.* (1992) and Rosenzweig and Kopelman (1995)

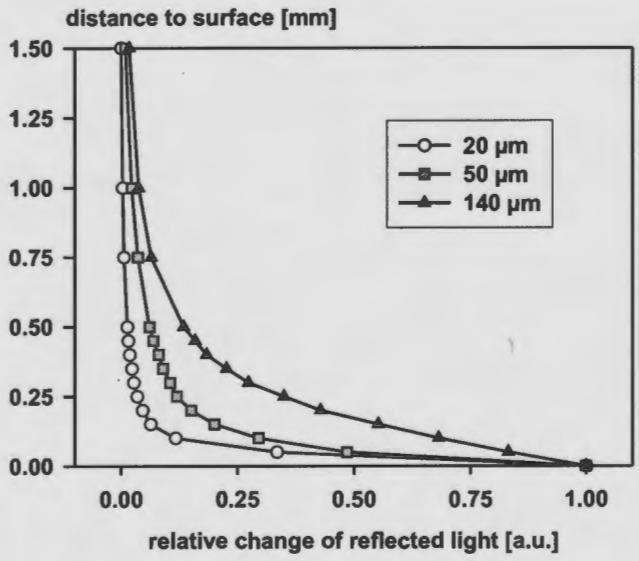

Figure 7.24 Results of surface detection measurements obtained by surface detection microprobes with different tip diameters (see legend box).

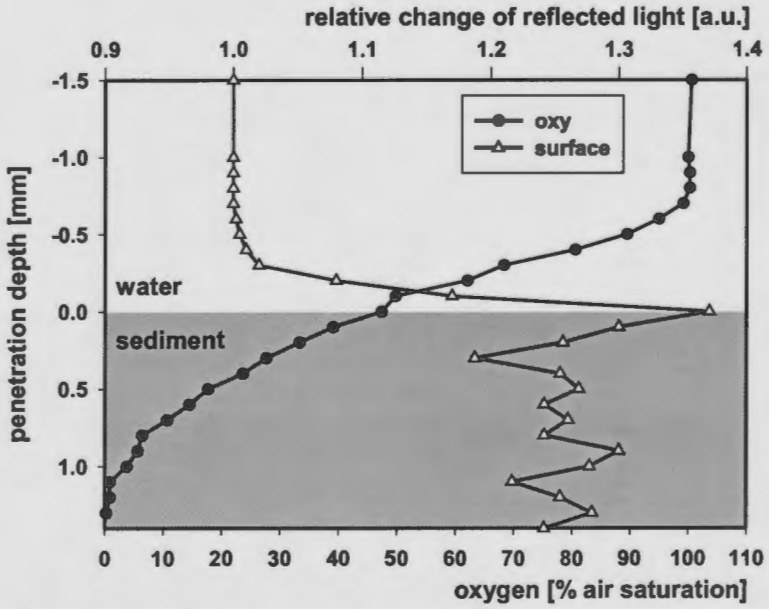

Figure 7.25 Oxygen depth profile and surface detection measurement of a microsensor combination made of an oxygen microoptode (oxy) and a surface detection microprobe (surface).

by adapting a technique which was already successfully used in near field microscopy. Silica single mode fibres with a core diameter of a few micrometers and a cladding diameter of 125 μm were tapered in a CO_2 laser beam to extremely thin tips. The diameter of the fibre tip and the form of the taper is controlled by the pulling velocity during the heating process and the heat itself via the intensity of the laser beam. Fibre tips down to 100 nm were produced with this technique. Then, the taper was coated with a reflective aluminium layer to ensure that the excitation light leaves the nanosensor only via its tip. The appropriate indicator was immobilised using a procedure described by Munkholm *et al.* (1986), where the fluorescent indicator is covalently cross linked in an UV curing polyacryl amid matrix using intense UV-illumination via the optical fibre itself. In this way, Kopelman *et al.* have developed fibre optic microsensors for the measurement of various parameters such as pH, O_2, glucose and ionic species like Ca^{2+}, potassium or nitrate. The pH and Ca^{2+} nanosensors, in particular, are very powerful tools for intracellular measurements (Barker *et al.*, 1998; Rosenzweig and Kopelman, 1995; Shortreed *et al.*, 1996a, b; Tan *et al.*, 1992).

The experimental set-up for working with sub-micron optodes consists of the following key components: a laser light source (for efficient coupling of excitation light into the single mode fibre), the coated tapered fibre with the sensing layer, a microscope and a photomultiplier tube. The optical fibre only acts as carrier for the excitation light (see Figure 7.26c). The fluorescence signal is collected by the lens optic of a microscope and guided to the detector. Therefore, applications are limited to samples which are almost clear and transparent and can only be performed on a microscope table. Significant losses may be caused by scattering or intrinsic absorption in the sample itself. The major potential of submicron optodes are intracellular measurements (Shortreed *et al.*, 1996b), where nano optodes are a real alternative to fluorescence microscopy techniques. Due to their small size, nano optodes can penetrate the cell wall without destroying the cell. Furthermore, injection of a luminophore, which may interfere with the cellular processes, can be avoided.

7.6 MEASURING SYSTEMS FOR OPTICAL MICROSENSORS AND MICROPROBES

In general, light of a specific light wavelength has to be guided to the fibre tip and interact in the sensing layer within an analyte. The modified or generated light has to be returned up the same fibre to be detected and further processed. Optical microsensors and microprobes are based on a single optical fibre, which serves as light guide in one or both directions. Therefore, the essential elements of the optical set-up are the optical coupling, the light source, and the detector. Once the electrooptical set-up is defined, the measuring method with appropriate evaluation schemes determines the measuring system with its resolution and precision.

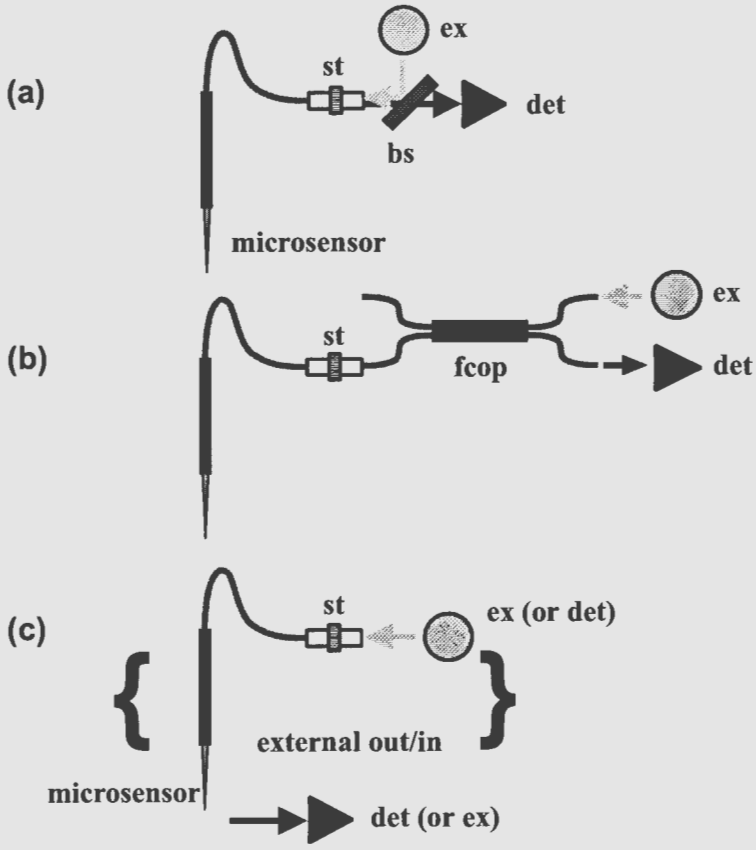

Figure 7.26 Schematic comparison of different electrooptical set-ups for optical microsensors: (a) bs – beamsplitter, det – photo detector, ex – excitation light source, st – standard fibre connectors; (b) fcop – 2 × 2 fibre coupler, det – photo detector, ex – excitation light source, st – standard fibre connectors; and (c) external in or out-coupling of light signal, means either (as shown) external detection, det – photo detector, ex – excitation light source, st – standard fibre connectors, or (not shown) external in-coupling.

7.6.1 Electrooptical Set-up: Light Sources

Light sources for optical microsensors range from natural sources, like sunlight (for spectrographic investigations), bio- and chemo-luminescence through to artificial sources: flash lamps, arc lamps, halogen lamps, lasers, laser diodes (LD) and light emitting diodes (LED). Because of their broad spectra and high light output, lamps are generally used in spectrographic measuring instruments where monocromators or variable optical filters select specific wavelengths that should be used for the measurement. In contrast, in most microsensor systems

lasers, LD's and LED's are used. This is due to either the high light output power and the inherent wavelength selectivity of lasers and LD's, or the low price and simplicity of LED's. Developments within the last few years have further improved the quality of the LED's especially concerning light output – even towards the blue end of the spectrum. Furthermore, LED's are stable long-term and have smaller power requirements than lasers or laser diodes. Because all semiconductor light sources are primarily used in the (optical) telecommunications industry, there is a vast range of standard fixings and connectors for coupling light in optical fibres. So, adaption or modification for specific measuring system is easy.

In optical microprobe projects, sunlight (or a lamp with a broad wavelength range) is used if whole spectra need to be measured, while a near infra-red (NIR) LD is used for surface detection. The measuring systems for microoptodes use LED's and appropriate optical filters as light sources. Both LD's and LED's are mounted using standard receptacles to facilitate interconnection. If the coupling efficiency needs to be increased additional lenses, such as ball or gradient refraction index lenses, can be used to image the light generating chip of the LD or LED to the fibre core. Alternatively the chips can be placed as near as possible to the fibre or they can be purchased with a fibre already attached, so-called "pig-tail" solutions.

7.6.2 Couplers

The first coupling elements were standard devices from the telecommunication industry: melting and grinded couplers (Figure 7.26b). In the first, the cladding of two fibres is partly removed, the fibres are twisted together, softly melted, stabilised with a polymer and, for mechanical robustness, fixed in a (steel tube or plastic) casing. Most of these are 2 × 2 couplers. In the second, the fibres are cut, ground to a fixed angle and then glued together, resulting in two half fibres sharing a common diameter. This glued assembly is fixed to a single fibre, which results in a 1 × 2 coupler. In newer couplers, light is transmitted more efficiently using gradient refraction index lenses (GRIN). All fibre-based couplers (Figure 7.26b) have a high directivity and the light distribution of the output branches can be manipulated to a certain extent (splits of 10:90 or 50:50, for example). Commercially available fibre couplers are supplied with connectors, do not need additional adjustments, they are are rugged, and they do not exhibit any change in performance over time. Despite their high quality and low price, fibre optics sometimes generate certain problems in sensing applications

(1) Availability. If a special type of silica fibre with a non-standard diameter is required, it might either be impossible (or very expensive) to get an appropriate coupler.
(2) Background noise. As the telecommunications only works with three wavelengths, 850 nm, 1.3 μm and 1.55 μm, all fibre optics are usually optimised for

use at these wavelengths. When applied to luminescence detection, the blue excitation light source also excites many of the epoxy glues that are used for fixing the coupler in the casing and the white dyes used in ceramics of the connector ferrule. This causes additional and unwanted luminescence, that can be larger than the signal. Therefore, couplers have to be carefully chosen.

The second possible coupler is a beam-splitter (Figure 7.26a). This coupler needs a carefully adjusted mechanical set-up to couple the light efficiently. The directivity can be improved by optical surface filters, e.g. the replacement of the common prism by a dichroic mirror. But, this is only possible if input and output wavelengths are sufficiently distinct for these mirrors, which usually have weak optical blocking properties. Additionally, any necessary optical filters must have a high blocking efficiency because they are the only means to prevent the intense excitation wavelengths from reaching the detector.

Finally, external coupling (Figure 7.26c) can be treated as an set-up bound "coupler". Here the fibre of the sensor is used as a light guide in one direction only. This either means the transmission of the exciting light (Tan *et al.*, 1992; Rosenzweig and Kopelman, 1995) to the microsensor or the return of captured light to the detector (radiance and irradiance microprobes). The former needs an external collection of light e.g. by a microscope lens and couples the light via a beam-splitter to a detector, while the latter has a broad illumination of the sample, e.g. by sun light or a halogen lamp, to measure the spectral information coming from the specific microsensor tip (Figure 7.18).

Various microoptode measuring systems (Klimant *et al.*, 1995; Holst *et al.*, 1995; Holst *et al.*, 1997; Kohls *et al.*, 1997) have used 2 × 2 melting couplers with silica fibres, similar in size and refraction index to the microoptodes themselves, while recent investigations also give promising results with a beamsplitter. All microprobes with 2 × 2 fibre couplers (except for surface detection and local luminescence measurements) utilise external in-coupling.

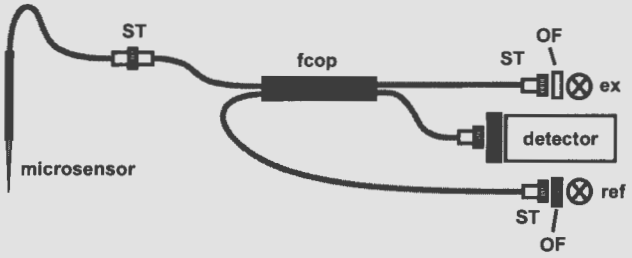

Figure 7.27 Schematic drawing of the electrooptical set-up of the measuring system for oxygen and temperature microoptodes: fcop – 2 × 2 fibre coupler; detector – photomultiplier tube; ex – excitation light source (LED, $\lambda p = 505\,nm$); ST – standard fibre connectors; OF – optical filters for excitation, emission and attenuation; ref – reference light source (LED, $\lambda p = 620\,nm$).

7.6.3 Detectors

The detectors for light captured by the tip of an optical microsensor have to be very sensitive, because the amount of light is very small. The most sensitive detectors are photomultiplier tubes (PMT). Based on photo-induced electron amplification, they are highly sensitive in the ultraviolet and visible spectral range but can only be used up to a maximum of 800 nm. Although currently available PMT's contain on-board high voltage power supply and current-to-voltage conversion circuits, they are expensive, very sensitive towards too much light, highly temperature dependent, and have a distinctive noise behaviour due to the amplification process. The second commonly used detectors are semiconductor avalanche photodiodes (APD), which are usefully sensitive from 500–900 nm. They are fast, need to be thermostated and have a noise behaviour like a PMT but with a lower sensitivity in the visible range. Finally, there are photodiodes, which are low in noise and temperature dependency, sensitive from 500–900 nm, slower in response time compared to an APD and cheap. APD's have better sensitivities than photodiodes due to the avalanche amplification process. PD-arrays or charge coupled devices, that are often used for spectrometers, principally show a behaviour comparable to PDs.

In nearly all optical microsensor applications PMTs have been used as detectors because the light power usually is in the range of pW. Nevertheless, improvements in sensor chemistry, optical set-ups and light sources will see PDs being used more in the future. This is preferable because of their better noise behaviour, higher stability and (not least) their cost. The exception is given by the described surface detection, that already uses PDs as detectors.

7.7 LIGHT INTENSITY BASED MEASURING METHODS AND SYSTEMS

In spectrographic measurements the collected light is measured in relation to its wavelength. The light captured by the microsensor tip is guided through the fibre, passes either a variable optical filter or a monochromator and reaches a sensitive detector like a PMT, or reaches an optical grating where the light is diffracted across an array of photodiodes or a line CCD-chip. In all these applications the measured spectra are compared to a reference spectrum measured before or after the excitation light source. This light source has to be very stable because any spectrally varying influence along the light path (extreme bending of the fibre, for instance) can not be referenced. In addition, external light "noise" would have to be measured separately with an identical detection path to enable sample beam referencing, or the light source and the detection would have to be modulated to separate the spectra from ambient light. For these reasons, most of these measurements are performed under defined and exact light conditions.

Another class of sensing applications are where a change in absorption spectra (or luminescence spectra of an immobilised indicator molecule) characterises the

sensing event. To employ these chemical sensors as microsensors it is necessary to make them insensitive towards indirect environmental changes e.g. change in ambient light, change of external absorption or refraction index, bending of the fibre etc.

There are two possible strategies to reduce problems due to ambient or stray light: time-multiplex beam referencing (measurement with and without the light signal and subtracting to resolve the intensity information of interest) and frequency modulation of the signal (sinusoidal or squarewave, and domain resolution through electronic filtering). The latter can be of advantage because it reduces the necessary bandwidth, and therefore the noise, of the measuring system. Extra care is needed to ensure the stability of the amplitude of the light signal that excites (or is absorbed by) the indicator at the microsensor tip.

For absolute intensity measurements only ratioing can reference changes in the optical environment that may potentially influence the light guiding property of the microsensor fibre and the sensor tip. Either light at two wavelengths is used for excitation and detection (time multiplex with one detector, or two different detectors) or two wavelengths are separately measured with two detectors. Then by ratioing all influences on the transmitted light the absolute intensity can be calculated (assuming that the influences are the same for the two wavelengths). Another solution is the optical separation of the sensing event from the environment, e.g. by an optical insulation of the sensor tip (Klimant *et al.*, 1995) and a fixation of the fibre (lander set-up).

One advantage of intensity-based measuring systems is their relative simplicity (Gruber *et al.*, 1993). The first measuring system for oxygen microoptodes (Klimant *et al.*, 1995) was intensity based with an amplitude modulation (rectangular signal). The light output of the excitation source, a blue LED ($\lambda = 450$ nm), was measured and controlled, and, to be independent of all optical properties of the environment, the microoptodes were optically insulated. Based on this first prototype, a small unit was developed for benthic landers which resulted in the first lander applications in shallow water (Glud *et al.*, 1998) and deep sea (Wenzhöfer *et al.*, 1998).

Surface detection systems (Klimant *et al.*, 1998) also detect light intensity. Here the influence of bending of the fibre is of minor importance as the biggest change in signal is from the surface being detected, unless the fibre is near to fracture. As shown in Figure 7.28 the system consists of a modulated ($f_{mod} = 10$ kHz) excitation light source, a laser diode ($\lambda = 780$ nm), a 2×2 silica fibre coupler (that is used as 2×1 coupler) and a PIN photodiode as detector. The unused branch of the coupler is immersed in oil to reduce unwanted reflection from the fibre end face. The analogue signal, which is displayed and present at the output (Figure 7.28), is directly proportional to the amount of reflected and backscattered light.

The measuring system for pH microoptodes is also intensity based. As the measuring scheme uses absorption based indicators, the measurement relies on the amount of reflected and backscattered excitation light. The excitation light is amplitude modulated ($f_{mod} = 1$ kHz) and, with a fibre optical 1×2 switch, two different LEDs were alternately used for the measurement, at wavelengths

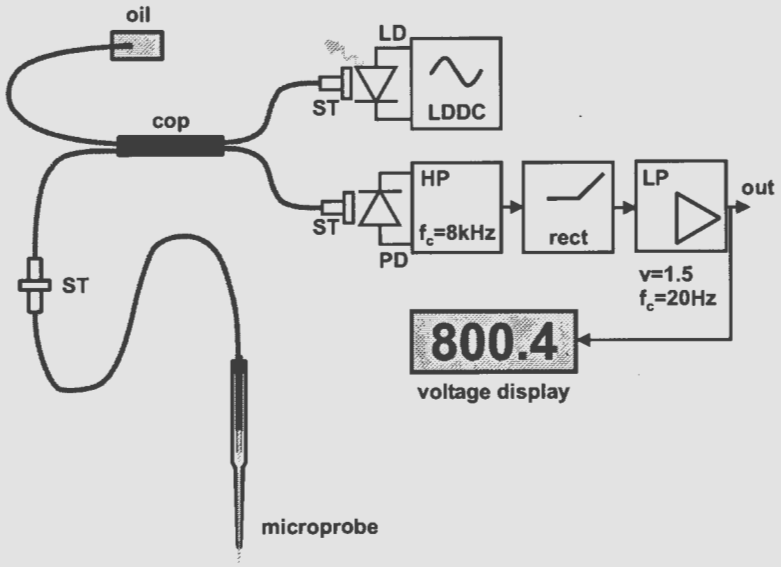

Figure 7.28 Schematic overview of light intensity based measuring system for surface detection: oil – one branch of the fibre coupler is immersed in oil to prevent fibre end face reflection; cop – 2 × 2 fibre coupler; ST – standard fibre connectors; LD – laser diode; LDDC – laser diode driving circuit, controls light output and modulates at 10 kHz; PD – PIN photodiode; HP – electronical highpass filter; fc – cut-off frequency; rect – precision rectifier; v – amplification; out – signal output in Volts.

$\lambda_1 = 470\,\text{nm}$ and $\lambda_2 = 595\,\text{nm}$. By a ratioing method the pH can be evaluated independent of changes in optical pathlength and the optical environment.

7.8 LIGHT-TIME BASED MEASURING METHODS AND SYSTEMS

Many interactions between light and molecules not only influence absorption or emission properties, but also influence the rates – a time parameter that describes the transition probability between different energy levels. A well known class of molecules include the luminescent O_2 indicators, which by dynamic quenching of their luminescence change both the emitted intensity as well as the time parameter that characterises the decay curve, the luminescence decay lifetime. This parameter does not depend on the indicator concentration, dye leaching or photo-bleaching (if the effect does not generate compounds that interact with the indicator), and it does not depend on the optical environment or the light path. Therefore, luminescence decay lifetimes are independent of influences such as: fibre bending, refraction index change, absorption change and so on.

There are two pathways to evaluate the time parameter, a measurement in the time domain: pulse decay, and phase modulation (measurement in the frequency

domain). They are equivalent but each has technical and practical advantages and disadvantages. Figure 7.29 compares the timing of the corresponding excitation (Figure 7.29, ex) and the luminescence emission (Figure 7.29, lum) signal. A luminophore with a single exponential decay curve is assumed.

In the pulse-decay method (Figure 7.29a) the shape of the excitation light signal is a rectangular pulse. The luminescence rises at a constant rate until it reaches a steady state. When the excitation is switched off, the time measurement starts. When the intensity falls below 1/e times the intensity I_0 (Figure 7.29a, the intensity when the excitation reaches zero), the resulting pulse width is equal to the decay time. The electronic circuits for this method need to avoid additional impedance contributing to the decay curve – which can be a disadvantage concerning noise reduction. Furthermore, the separation of constant light compounds, that can be very high due to incoupled ambient light, is very difficult. Ambient effects need to be subtracted from the decay time and very early in the amplification stages of a measuring system. There are other techniques (Lippitsch *et al.*, 1988; Zhang *et al.*, 1993) to evaluate the luminescence lifetime in the time-domain: pulse excitation and level crossing (or integration) is common, for instance.

The phase modulation technique (Figure 7.29b) measures the luminescence lifetime in the frequency domain (Lakowicz, 1983; Gratton and Limkeman, 1984; Berndt and Lakowicz, 1992; Alcala *et al.*, 1995; Gruber *et al.*, 1995; Holst *et al.*, 1995). For that purpose the excitation light is sinusoidally modulated at a modulation frequency f_{mod}. The reaction is an emission of sinusoidal light, that is weaker in intensity and delayed compared to the excitation. This delay is called phase angle Φ between two sinusoidal signals and the relation to the luminescence lifetime τ is given (Lakowicz, 1983):

$$\tan(\Phi) = 2\pi \cdot f_{mod} \cdot \tau$$

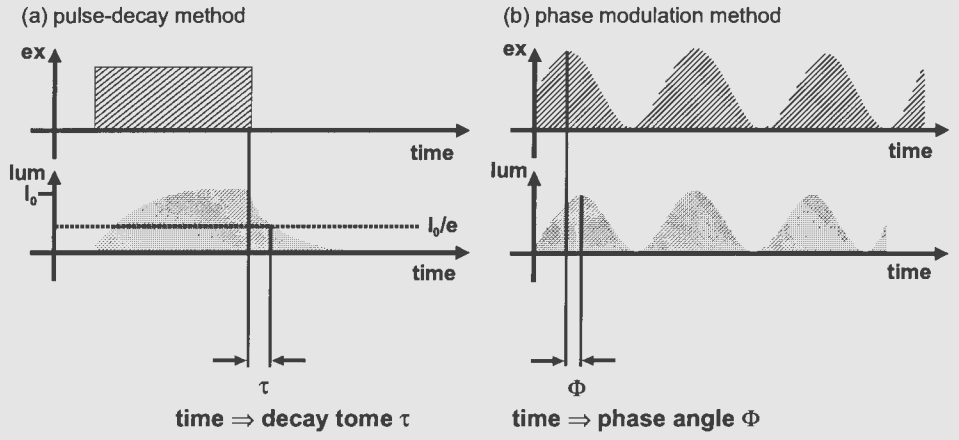

Figure 7.29 Timing relations of excitation and luminescence light signals for pulse-decay and phase modulation measurements.

If the two lifetimes τ_1 and τ_2, that describe the boundaries of the measuring range for the analyte, are known, the optimum modulation frequency f_{opt} can be derived to (Holst *et al.*, 1997):

$$f_{opt} = \frac{1}{2\pi \cdot \sqrt{\tau_1 \cdot \tau_2}}.$$

As the phase modulation technique uses a single frequency, the signal can be electronically filtered (with a narrow bandwidth) which simplifies the suppression of noise and constant/ambient light. Nevertheless, in both methods care has to be taken when referencing zero time, because all electronic components additionally influence the signal.

If there are more luminescent decay products, they can be time-domain resolved by measuring more points along the decay curve and (least squares) curve analysis. Alternatively, they can be resolved in the frequency domain, by measuring at multiple frequencies and spectral analysis (Lakowicz, 1983; Gratton and Limkeman, 1984). Whether the time parameter is measured in the time or the frequency domain finally depends on the specific application and the most convenient technical solution for the measuring system, since the information content is equivalent.

The measuring system for oxygen microoptodes uses the phase modulation technique to evaluate the oxygen dependent lifetime change of the applied indicators. The excitation light source, an LED ($\lambda_p = 505$ nm, Figure 7.27, ex), is sinusoidally modulated at frequencies of $f_{mod} = 1.25$ kHz, 5 kHz or 37.5 kHz (for different lifetime ranges). The light is coupled through a shortpass filter ($\lambda_c = 540$ nm, Figure 7.27, OF) into a 2 × 2 fibre coupler (Figure 7.27, fcop). One branch of the coupler is connected via a standard fibre connector (Figure 7.27, ST) with the microoptode. The other branch is used for referencing purposes (Figure 7.27, ref). The luminescence is guided back through the coupler via a longpass emission filter ($\lambda_c = 590$ nm) to the detector, a photomultiplier tube (Figure 7.27, detector). Alternately, the excitation LED (Figure 7.27, ex) and the reference LED (Figure 7.27, ref) are switched on and their (phase angle) difference is measured. Finally, the difference of both give the luminescence lifetime induced phase angle whereas electronic influences are cancelled out (except any difference between light sources). For the phase angle evaluation there are two possible solutions: (1) a zero-crossing detector (Holst *et al.*, 1995), which basically compares the zero crossing event of a reference and the measuring signal and converts the corresponding pulse width into a phase angle, and (2) a dual phase lock-in detector (Gruber *et al.*, 1995; Holst *et al.*, 1998) (Figure 7.30) that is better suited for PMT detectors.

As shown in Figure 7.30 the signal processing of a lock-in detector starts with the multiplication (in this case a demodulation) of the measuring signal that might been amplified and pre-filtered. The signal is multiplied both, with a reference sine- and cosine-signal of the same frequency f_{mod}. The products contain many different frequency contributions. If the product signals are now

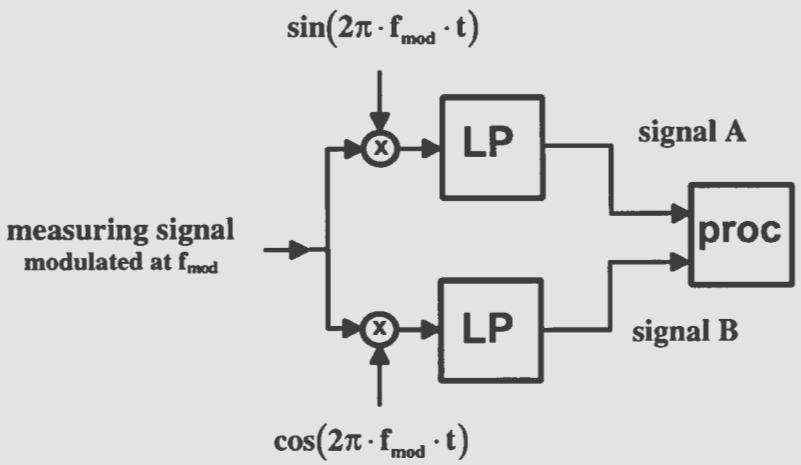

Figure 7.30 Principle of lock-in detection: fmod – modulation frequency; LP – electronical lowpass filter; proc – calculations that are explained in the text; signal A and B – output signals of the lowpass filters of the respective signal paths; x – multiplication.

lowpass filtered with a cut-off frequency much lower than f_{mod}, the resulting signals A and B (Figure 7.30, signal A, signal B) consist of the amplitudes of the measuring and the reference signals, and of the in-phase and quadrature angle between the measurment and reference signals. Therefore, the amplitude and the phase angle Φ of the measuring signal can be simply calculated (Figure 7.30, proc) by:

$$\text{amp} = \sqrt{(\text{signal})^2 + (\text{signal})^2}$$

$$\Phi = \arctan\left(\frac{\text{signal A}}{\text{signal B}}\right)$$

This method of phase angle evaluation is very precise and can resolve even very noisy signals. As this phase angle is measured for excitation light, Φ_{sig}, and reference light, Φ_{ref}, alternately, the real phase angle, caused by the luminescence lifetime, is the difference between: $\Phi_{lum} = \Phi_{sig} - \Phi_{ref}$.

Although the phase modulation technique has many advantages compared to intensity measurements there are noise events that can have a severe impact on the quality of the measurement. If there are additional luminescence signals that interfere with the analytical signal, the phase angle measured at a single frequency is the sum of both signals. Therefore, it not only depends on the phase angle of the indicator based signal but also on the ratio of both amplitudes – an intensity parameter. If the noise signal is constant, it can be separately measured and mathematically corrected. If it is variable, the measurement has to be made at multiple frequencies to obtain the correct information.

Despite the fact that they require more complex electronics compared to intensity based systems, light-time measuring systems reveal better and reliable results in conjunction with optical microsensors. However, their sensing principles depend on a change in a time parameter rather than on the intensity of the optical signal. Therefore, they have been to-date limited to oxygen and temperature, but will in the future be extended to pH and carbon dioxide measurements.

7.9 FROM MICRO TO MACRO SCALE

Historically, principles for optical sensing were used on large scales. The driving force for the developments and investigations came from biomedical applications (Lübbers and Opitz, 1975; Gehrich *et al.*, 1986; Tusa *et al.*, 1986; Leiner, 1991; Wolfbeis, 1991). These larger sensors, when they are made as sensing layers on transparent supports called planar optodes, can as well be applied in oceanography. They exhibit many advantages: high pressure and long-term stability, immunity to stirring effects etc.. Therefore, applications in the water column have already been reported (DeGrandpre, 1993) and are still a matter of research (Holst *et al.*, 1998, unpublished results). Systems have become cheaper, more reliable and stable and the preparation of the sensing layers is much easier. In contrast, due to diffusion effects the response time of physically larger sensors increases in proportion to surface area. As the sensing principle of all optical chemical sensors is diffusion based, spherical diffusion to a microsensor is reduced to a nearly one-dimensional diffusion for planar optodes. Consequently the diffusion boundary layer governs the response time of planar optodes.

Another potential application of large scale optodes has been presented (Glud *et al.*, 1996) and is continuously investigated (Holst *et al.*, 1998), mapping of two-dimensional oxygen distributions by planar oxygen optodes that are placed perpendicular to the sediment-water interface. This technique gives full access to the heterogeneity of the oxygen distribution in sediment and microbial communities, which previously could only be achieved by profiling measurements. Conclusively, optical chemical sensors have great potential for analytical measurements in oceanography.

References

Alcala, J.R., Liao, S.-C. and Zheng, J. (1995). Real Time Frequency Domain Fiberoptic Temperature Sensor, *IEEE Transactions on Biomedical Engineering*, 42, 471–476.

Amann, R. and Kühl, M. (1998). *In situ* methods for assessment of microorganisms and their activities, *Current Opinion in Microbiology*, in press.

Andrews, D. and Bennett, A. (1981). Measurements of Diffusivity Near the Sediment-Water Interface with a Fine-Scale Resistivity Probe, *Geochimica et Cosmochimica Acta*, 45, 2169–2175.

Bacon, J.R. and Demas, J.N. (1987). Determination of Oxygen Concentrations by Luminescence Quenching of a Polymer-Immobilized Transition-Metal Complex, *Analytical Chemistry*, 59, 2780–2785.

Baldini, F. and Del Bianco, A. (1992). Optical Fiber Sensor for Oxygen Detection Working on an Absorption Basis, *Fiber and Integrated Optics*, 11, 123–133.

Barker, S.L.R., Kopelman, R., Meyer, T.E. and Cusanovich, M.A. (1998). Fiber-Optic Nitric Oxide-Selective Biosensors and Nanosensors, *Analytical Chemistry*, 70, 971–976.

Bergman, I. (1986). Rapid-Response Atmospheric Oxygen Monitor Based on Fluorescence Quenching, *Nature*, 218, 396.

Berndt, K.W. and Lakowicz, J.R. (1992). Electroluminescent Lamp-Based Phase Fluorometer and Oxygen Sensor, *Analytical Biochemistry*, 201, 319–325.

Bishop, E. (1972). Indicators, New York: Pergamon Press.

Carraway, E.R., Demas, J.N., DeGraff, B.A. and Bacon, J.R. (1991). Photophysics and Photochemistry of Oxygen Sensors Based on Luminescent Transition-Metal Complexes, *Analytical Chemistry*, 63, 337–342.

Carraway, E.R., Demas, J.N. and DeGraff, B.A. (1991). Luminescence Quenching Mechanism for Microheterogenous Systems, *Analytical Chemistry*, 63, 332–336.

Carraway, E.R. and Demas, J.N. (1991). Photophysics and Oxygen Quenching of Transition-Metal Complexes on Fumed Silica, *Langmuir*, 7, 2991–2998.

Dakin, J. and Culshaw, B. (1988). Optical Fibre Sensors: I Principles and Components, II Systems and Applications, Artech House, Boston and London.

DeGrandpre, M.D. (1993). Measurement of Seawater pCO_2 Using a Renewable-Reagent Fiber Optic Sensor with Colorimetric Detection, *Analytical Chemistry*, 65, 331–337.

Demas, J.N. (1976). Luminescence Decay Times and Bimolecular Quenching, *Journal of Chemical Education*, 53, 657–663.

Demas, J.N. and DeGraff, B.A. (1992). On the Design of Luminescence Based Temperature Sensors, *Proceedings SPIE*, 1796, 71–75.

Fukshansky-Kazarinova, N., Fukshansky, L., Kühl, M. and Jørgensen, B.B. (1997). General theory of three-dimensional radiance measurements with optical microprobes, *Applied Optics*, 36, 6520–6528.

Fukshansky-Kazarinova, N., Fukshansky, L., Kühl, M. and Jørgensen, B.B. (1998). Solution of the inverse problem of radiative transfer on the basis of measured internal fluxes, *Journal of Quantitative Spectroscopy and Radiation Transfer*, 59, 77–89.

Garcia-Pichel, F. (1995). A Scalar Irradiance Fiber-Optic Microprobe for the Measurement of Ultraviolet Radiation at High Spatial Resolution, *Photochemistry and Photobiology*, 61(3), 248–254.

Garcia-Pichel, F. and Bebout, B. (1996). Penetration of Ultraviolet Radiation into Shallow Water Sediments: High Exposure for Photosynthetic Communities, *Marine Ecology Progress Series*, 131, 257–262.

Gehrich, J.L., Lübbers, D.W., Opitz, N., Hansmann, D.R., Miller, W.W., Tusa, J.K. and Yafuso, M. (1986). Optical Fluorescence and its Application to an Intravascular Blood Gas Monitoring System, *IEEE Transactions on Biomedical Engineering*, 33, 117–121.

Glud, R.N., Klimant, I., Holst, G., Kohls, O., Meyer, V., Kühl, M. and Gundersen, J.K. (1997). Adaptation, test and *in situ* measurements with O_2 microopt(r)odes on benthic landers, *Deep sea Research*, (subm. f. publ.).

Glud, R.N., Ramsing, N.B., Gundersen, J.K. and Klimant, I. (1996). Planar Optrodes: a New Tool for Fine Scale Measurements of Two-Dimensional O_2 Distribution in Benthic Communities, *Marine Ecology Progress Series*, 140, 217–226.

Grattan, K.T.V. and Zhang, Z.Y. (1995). Fiber Optic Fluorescence Thermometry, London Chapman & Hall.

Gratton, E. and Limkeman, M. (1984). Resolution of Mixtures of Fluorohores Using Variable-Frequency Phase and Modulation Data, *Biophysical Journal*, 46, 479–486.

Green, T.J., Wilson, D.F., Vanderkooi, J.M. and Defeo, S.P. (1988). Phosphorimeters for Analysis of Decay Profiles and Real Time Monitoring of Exponential Decay and Oxygen Concentrations, *Analytical Biochemistry*, 174, 73–79.

Gruber, W.R., Klimant, I. and Wolfbeis, O.S. (1993). Intrumentation for Optical Measurement of Dissolved Oxygen Based on Solid State Technology, *Proceedings SPIE*, 1885, 448–457.

Gruber, W.R., O'Leary, P. and Wolfbeis, O.S. (1995). Detection of Fluorescence Lifetime Based on Solid State Technology and its Application to Optical Oxygen Sensing, *Proceedings SPIE*, 1885, 448–457.

Hales, B., Burgess, L. and Emerson, S. (1997). An Absorbance-Based Fiber-Optic CO_2 (aq) Measurement in Porewaters of Sea Floor Sediments, *Marine Chemistry*, 59, 51–62.

Hartmann, P. and Leiner, M.J.P. (1995). Luminescence Quenching Behavior of an Oxygen Sensor Based on a Ru(II) Complex Dissolved in Polystyrene, *Analytical Chemistry*, 67, 88–93.

Holst, G., Kühl, M. and Klimant, I. (1995). A Novel Measuring System for Oxygen Microoptodes based on Phase Modulation Technique, *Proceedings SPIE*, 2508, 387–398.

Holst, G., Kühl, M., Klimant, I., Liebsch, G. and Kohls, O. (1997). Characterization and Application of Temperature Microoptodes for Use in Aquatic Biology, *Proceedings SPIE*, 2980, 164–170.

Holst, G., Glud, R. N., Kühl, M. and Klimant, I. (1997). A Microoptode Array for Fine-Scale Measurement of Oxygen Distribution, *Sensors and Actuators B*, 38–39, 122–129.

Holst, G., Kohls, O., Klimant, I., König, B., Kühl, M. and Richter, T. (1998). A Modular Luminescence Lifetime Imaging System for Mapping Oxygen Distribution in Biological Samples, *Sensors and Actuators B*, (subm. f. publ.).

Jørgensen, B.B. and Des Marais, D.J. (1986). A simple fiber-optic microprobe for high resolution light measurements: application in marine sediment, *Limnology and Oceanography*, 31, 1376–1383.

Kautsky, H. (1939). Quenching of Luminescence by Oxygen, *Transactions of Faraday Society*, 35, 216–219.

Karsten, U. and Kühl, M. (1996). Die Mikrobenmatte – das kleinste ökosystem der Welt, *Biologie in unserer Zeit*, 26, 16–26.

Khalil, G.-E., Gouterman, M. and Green, E. (1988). Method and Sensor for Measuring Oxygen Concentration, In United States Patent, Abbott Laboratories, USA, 23.

Klimant, I., Belser, P. and Wolfbeis, O.S. (1992). Novel Longwave Absorbing and Emitting Transition Metal Complexes for Use in Optical Oxygen Sensing, In Europt(r)ode I, Graz, 1.

Klimant, I., Meyer, V. and Kühl, M. (1995). Fiber-Optic Oxygen Microsensors, a New Tool in Aquatic Biology, *Limnology & Oceanography*, 40, 1159–1165.

Klimant, I., Holst, G. and Kühl, M. (1995). Oxygen Microoptodes and their Application in Aquatic Environment, *Proceedings, SPIE*, 2508, 375–386.

Klimant, I., Kühl, M., Glud, R.N. and Holst, G. (1997). Optical Measurement of Oxygen and Temperature in Microscale: Strategies and Biological Applications, *Sensors and Actuators B*, 38, 29–37.

Klimant, I., Holst, G. and Kühl, M. (1998). A Simple Fiberoptic Sensor to Detect the Penetration of Microsensors into Sediments and other Biogeochemical Systems, *Limnology & Oceanography*, 42, (in print).

Kohls, O., Klimant, I., Holst, G. and Kühl, M. (1997). Development and Comparison of pH Microoptodes for Use in Marine Systems, *Proceedings SPIE*, 2978, 82–93.

Kühl, M. and Jørgensen, B.B. (1992). Spectral Light Measurements in Microbenthic Phototrophic Communities with a Fiber-Optic Microprobe Coupled to a Sensitive Diode Array Detector, *Limnology & Oceanography*, 37, 1813–1823.

Kühl, M., Lassen, C. and Jørgensen, B.B. (1994a). Optical Properties of Microbial Mats: Light Measurements with Fiber-Optic Microprobes, In: Microbial Mats: Structure, Development, and Environmental Significance (Stal, L.J. and Caumette, P., eds), Springer, Berlin, 149–167.

Kühl, M., Lassen, C. and Jørgensen, B.B. (1994b). Light Penetration and Light Intensity in Sandy Marine Sediments Measured with Irradiance and Scalar Irradiance Fiber-Optic Microprobes, *Marine Ecology Progress Series*, 105, 139–148.

Kühl, M., Glud, R.N., Ploug, H. and Ramsing, N.B. (1996). Microenvironmental Control of Photosynthesis and Photosynthesis-Coupled Respiration in an Epilithic Cyanobacterial Biofilm, *Journal of Phycology*, 32, 799–812.

Kühl, M., Lassen, C. and Revsbech, N.P. (1997). A Simple Light Meter for Measurements of PAR (400 to 700 nm) with Fiber-Optic Microprobes: Application for P vs E_0 (PAR) Measurements in a Microbial Mat, *Aquatic Microbial Ecology*, 13, 197–207.

Kühl, M. and N.P. Revsbech (1998). Microsensor for the Study of Interfacial Biogeochemical Processes. In: Boudreau, B.P. and Jørgensen, B.B. (eds), The Benthic Boundary Layer, Oxford University Press, Oxford, (in press).

Lakowicz, J.R. and Cherek, H. (1981). Phase-Sensitive Fluorescence Spectroscopy: A New Method to Resolve Fluorescence Lifetimes or Emission Spectra of Components in a Mixture of Fluorophores, *Journal of Biochemical and Biophysical Methods*, 5, 19–35.

Lakowicz, J.R. and Balter, A. (1982). Analysis of Excited-State Processes by Phase-Modulation Fluorescence Spectroscopy, *Biophysical Chemistry*, 16, 117–132.

Lakowicz, J.R. (1983). Principles of Fluorescence Spectroscopy, New York: Plenum Press.

Lakowicz, J.R. and Maliwal, B.P. (1985). Construction and Performance of a Variable-Frequency Phase-Modulation Fluorometer, *Biophysical Chemistry*, 21, 61–78.

Lakowicz, J.R. and Szmacinski, H. (1993). Fluorescence Lifetime-Based Sensing of pH, Ca^{2+}, K^+ and Glucose, *Sensors and Actuators B*, 11, 133–143.

Lassen, C., Ploug, H. and Jørgensen, B.B. (1992). A Fibre-Optic Scalar Irradiance Microsensor: Application for Spectral Light Measurements in Sediments, *FEMS Microbiology Ecology*, 86, 247–254.

Lassen, C. and Jørgensen, B.B. (1994). A Fiber-Optic Irradiance Microsensor (Cosine Collector): Application for *In Situ* Measurements of Absorption Coefficients in Sediments and Microbial Mats, *FEMS Microbiology Ecology*, 15, 321–336.

Leiner, M.J.P. (1991). Luminescence Chemical Sensors for Biomedical Applications: Scope and Limitations, *Analytica Chimica Acta*, 225, 209–222.

Lippitsch, M.E., Pusterhofer, J., Leiner, M.J.P. and Wolfbeis, O.S. (1988). Fibre-Optic Oxygen Sensor with the Fluorescence Decay Time as the Information Carrier, *Analytica Chimica Acta*, 205, 1–6.

Lübbers, D.W. and Opitz, N. (1975). Die pCO_2/pO_2-Optode: eine neue pCO_2- bzw. pO_2-Messonde zur Messung des pCO_2 oder pO_2 von Gasen und Flüssigkeiten, *Zeitschrift für Naturforschung C*, 30, 532–533.

Lübbers, D.W., Opitz, N., Speiser, P.P. and Bisson, H.J. (1977). Nanoencapsulated Fluorescence Indicator Molecules Measuring pH and pO_2 Down to Submicroscopical regions on the Basis of the Optode-Principle, *Zeitschrift für Naturforschung C*, 32, 512–1–512–2.

MacCraith, B.D., O'Keefe, G., McDonagh, C. and McEvoy, A. (1994). LED-based fibre optic oxygen sensor using sol-gel coating, *Electronics Letters*, 30 (11), 888–889.

McDonagh, C., MacCraith, B.D. and McEvoy, A.K. (1998). Tailoring of Sol-Gel Films for Optical Sensing of Oxygen in Gas and Aqueous Phase, *Sensors and Actuators B*, 70, 45–50.

Mills, A. and Chang, Q. (1993). Fluorescence Plastic Thin-Film Sensor for Carbon Dioxide, *Analyst*, 118, 839–843.

Munkholm, C., Walt, D., Milanovich, F. and Klainer, S. (1986). Polymer Modification of Fibre Optic Chemical Sensors as a Method for Enhancement of Signals for pH Measurement, *Analytical Chemistry*, 58, 1427–1430.

Munkholm, C., Walt, D.M. and Milanovich, F.P. (1988). A Fiber Optic Sensor for Carbon Dioxide, *Talanta*, 35, 109–114.

Papkovsky, D.P., Olah, J. and Kurochkin, H.N. (1993). Fibre-Optic Lifetime-Based Enzyme Biosensor, *Sensors and Actuators B*, 11, 525–530.

Peterson, I. and Fitzgerald, R.V. (1984). Fiber-Optic Probe for *In Vivo* Measurement of Oxygen Partial Pressure, *Analytical Chemistry*, 56, 62–67.

Revsbech, N.P., Jørgensen, B.B., Blackburn, T.H. and Cohen, Y. (1983). Microelectrode studies of photosynthesis and O_2, H_2S, and pH profiles of a microbial mat, *Limnology & Oceanography*, 28, 1062–1074.

Revsbech, N.P. and Jørgensen, B.B. (1986). Microelectrodes: their Use in Microbial Ecology, *In Advances in Microbial Ecology*, Plenum Publishing Corporation.

Revsbech, N.P. (1989). An Oxygen Microelectrode with a Guard Cathode, *Limnology & Oceanography*, 34, 474–478.

Revsbech, N.P. (1994). Analysis of Microbial Mats by Use of Electrochemical Microsensors: Recent Advances, In: Microbial mats: Structure, Development, and Environmental Significance (Stal, L.J. and Caumette, P., eds), Springer, Berlin, 135–147.

Robert-Baldo, G.L., Morris, M.J. and Byrne, R.H. (1987). Fibre-Optic pH sensor for seawater monitoring, *Proceedings SPIE*, 798, 294–301.

Rosenzweig, Z. and Kopelman, R. (1995). Development of a Submicrometer Optical Fiber Oxygen Sensor, *Analytical Chemistry*, 67, 2650–2654.

Sacksteder, L.A., Demas, J.N. and DeGraff, B.A. (1993). Design of Oxygen Sensors based on Quenching of Luminescent Metal Complexes: Effect of Ligand Size on Heterogeneity, *Analytical Chemistry*, 65, 3480–3483.

Schreiber, U., Kühl, M., Klimant, I. and Reising, H. (1996). Measurement of Chlorophyll Fluorescence within Leaves Using a Modified PAM Fluorometer with a Fiber-Optic Microprobe, *Photosynthesis Research*, 47, 103–109.

Severinghaus, J.W., Bradley, A.F. (1958). Electrodes for blood P_{O_2} and P_{CO_2} Determination, *Journal of Applied Physiology*, 13, 515–520.

Sharma, A. and Wolfbeis, O.S. (1988). Fiberoptic Oxygen Sensor Based on Fluorescence Quenching and Energy Transfer, *Applied Spectroscopy*, 42, 1009–1011.

Sipior, J., Bambot, S., Romauld, M., Carter, G.M., Lakowicz, J.R. and Rao, G. (1995). A Lifetime-Based Optical CO_2 gas sensor with Blue or Red Excitation and Stokes or Anti-Stokes Detection, *Analytical Biochemistry*, 227, 309–318.

Shortreed, M., Bakker, E. and Kopelman, R. (1996). Miniature Sodium-Selective Ion-Exchange Optode with Fluorescent pH Chromoionophores and Tunable Dynamic Range, *Analytical Chemistry*, 68(15), 2656–2662.

Shortreed, M., Kopelman, R. Kuhn, M. and Hoyland, B. (1996). Fluorescent Fiber-Optic Calcium Sensor for Physiological Measurements, *Analytical Chemistry*, 68(8), 1414–1418.

Stern, O. and Volmer, M. (1919). Über die Abklingzeit der Fluoreszenz, *Physikalische Zeitschrift*, 20, 183–188.

Tan, W., Shi, Z.-Y., Smith, S., Birnbaum, D. and Kopelman, R. (1992). Submicrometer Intracellular Chemical Optical Fiber Sensors, *Science*, 258, 778–781.

Tengberg, A., De Bovee, F., Hall, P., Berelson, W., Chadwick, D., Ciceri, G. *et al.* (1995). Benthic Chamber and Profiling Landers in Oceanography – A Review of Design, Technical Solutions and Functioning, *Progress in Oceanography*, 35, 253–294.

Tusa, J.K., Hacker, T., Hansmann, D.R., Kaput, T.M. and Maxwell, T.P. (1986). Fiber Optic Microsensor for Continous *In-Vivo* Measurement of Blood Gases, *Proceedings SPIE*, 713, 137–143.

Vanderkooi, J.M., Maniara, G., Green, T.J. and Wilson, D.F. (1987). An Optical Method for Measurement of Dioxygen Concentration Based upon Quenching of Phosphorescence, *Journal of Biological Chemistry*, 262, 5476–5482.

Vogelmann, T.C. and Björn, L.O. (1984). Measurement of Light Gradients and Spectral Regime in Plant Tissue with a Fibre Optic Probe, *Physiologia Plantarum*, 60, 361–368.

Wenzhöfer, F., Kohls, O. and Holby, O. (1998). Deep Penetration of Oxygen Measured *in situ* by Oxygen Optodes, *Deep-Sea Research*, (subm. f. publ.).

Wilson, D.F., Vanderkooi, J.M., Green, T.J., Maniara, G., Defeo, S.P. and Bloomgarden, D.C. (1987). A Versatile and Sensitive Method for Measuring Oxygen, In Oxygen Transport To Tissue IX, New York: Plenum Press, 71–77.

Wolfbeis, O.S., Offenbacher, H., Kroneis, H. and Marsoner, (1984). A Fast Responding Fluorescence Sensor for Oxygen, *Mikrochimica Acta*, I, 153–158.

Wolfbeis, O.S., Leiner, M.J.P. and Posch, H.E. (1986). A New Sensing Material for Optical Oxygen Measurement, with the Indicator Embedded in an Aqueous Phase, *Mikrochimica Acta, III*, 359–366.

Wolfbeis, O.S., Weiß, L.J., Leiner, M.J.P. and Ziegler, W. (1988). Fiber-Optic Fluorosensor for Oxygen and Carbon Dioxide, *Analytical Chemistry*, 60, 2028–2030.

Wolfbeis, O.S. (1991). Fiber Optic Chemical Sensors and Biosensors, CRC Press, Boca Raton.

Wolthuis, R.A., McCrae, D., Saaski, E., Hartl, J. and Mitchell, G. (1992). Development of a Medical Fiber-Optic pH Sensor Based on Optical Absorption, *IEEE Transactions on Biomedical Engineering*, 39, 531–537.

Zhang, Z., Grattan, K.T.V. and Palmer, A.W. (1993). Phase-Locked Detection of Fluorescence Lifetime and its Thermometric Applications, *Proceedings SPIE*, 1885, 228–239.